

Supporting Information

for

The side-arm effect controlled stereodivergent polymerization of 1-butene

Guangyu Zhu,^{‡a,b} Liang Wang, ^{‡a,b} Wenjie Tao,^{*,a,b,c} Hongbin Hou,^{a,b} Guangqiang

Xu,^{a,b,c} Bo Wang,^{a,b} Qinggang Wang,^{*,a,b,c}

^a Key Laboratory of Photoelectric Conversion and Utilization of Solar Energy, Qingdao Institute of Bioenergy and Bioprocess Technology, Chinese Academy of Sciences, Qingdao 266101, China.

^b Shandong Energy Institute, Qingdao 266101, China.

^c Center of Materials Science and Optoelectronics Engineering, University of Chinese Academy of Sciences, Beijing 100049, China.

[‡] These authors contributed equally to this work.

*Corresponding authors: Wenjie Tao (E-mail: taowj@qibebt.ac.cn), Qinggang Wang (wangqg@qibebt.ac.cn).

Table of content	Page Number
1. Experimental Section	S1
2. Supplementary Table	S4
3. Synthesis and NMR Data of Ligands L6a–L6e	S5
4. Synthesis and NMR Data of Tridentate [O-NX] Titanium Complexes 6a–6e	S13
5. NMR Spectra of Polymers	S22
6. GPC Traces of Polymers.....	S26
7. DSC Data of Polymers.....	S35
8. WAXD data of Polymers	S38
9. Tensile-tests of Polymers	S41
10. Crystal Data	S43
References:.....	S47

1. Experimental Section

1.1 General.

All manipulations of oxygen/water sensitive materials were performed under a dry argon atmosphere using a glove-box or standard Schlenk techniques. Liquid 1-butene was purified by activated 4Å molecular sieves and stored in a pressure resistant bottle before use. All dry solvents were redistilled after collected from the solvent purification system and then stored over activated 4 Å molecular sieves in a glovebox. Deuterated solvents used for NMR spectroscopy were dried and distilled prior to use. Chromatographic tetrahydrofuran (THF) was purchased from Honeywell LTD for the analysis of GPC measurements. LDPE-2426H was purchased from CHN Energy Xinjiang Chemical Co. Ltd. All other chemicals were commercially available and used without appropriate purification. Reactions were monitored by thin layer chromatography (TLC) using silicycle pre-coated silica gel plates. Flash column chromatography was performed over silica gel (200-300 mesh).

1.2 Methods.

NMR

¹H NMR spectra were recorded on a Bruker AV-400 spectrometer in chloroform-d. Chemical shifts are reported in ppm with the internal chloroform signal at 7.26 ppm as a standard. The data are being reported as (s = singlet, d = doublet, t = triplet, m = multiplet or unresolved, brs = broad singlet, coupling constant(s) in Hz, integration). ¹³C NMR spectra were recorded on a Bruker AV-400 spectrometer in chloroform-d. Chemical shifts are reported in ppm with the internal chloroform signal at 77.0 ppm as a standard. The quantitative ¹³C NMR spectra of poly(1-butene)s were recorded according to known references.^{1,2}

GPC

Molecular weights (M_n s) and dispersities (\bar{D}) of the polymers were determined by gel permeation chromatography (GPC, Agilent 1260 LC, USA) using THF as the eluent (flow rate: 1 mL/min, at 40 °C) and the sample concentration was 1 mg/mL. The curve

was calibrated using monodisperse polystyrene standards covering the molecular weight range from 580 to 460000 Da.

XRD

X-Ray crystallographic data were collected using a Bruker AXSD8 X-ray diffractometer.

HRMS

High resolution mass spectra (HRMS) were carried out with a Bruker ESI-Q-TOF MS/MS.

EA

Elemental analysis (EA) was performed by the Analytical Laboratory of Shanghai Institute of Organic Chemistry (CAS).

DSC

Differential scanning calorimetry (DSC) measurements were performed on DSC 3500 Sirius. The temperature was calibrated with C₁₀H₁₆, indium, tin, bismuth and zinc standard. Measurements were performed under N₂ atmosphere with a flow rate of 20 mL/min. Each sample with a mass of 10 mg was used for the measurement. The typical procedures for the measurements of samples were as follows: in the first heating scan, samples were heated from -80 °C to 200 °C at a heating rate of 10 K/min. In the second heating scan, samples were cooled to -80 °C at 10 K/min and kept at -80 °C for 20 min to eliminate any thermal history, and subsequently reheated to 200 °C at 10 K/min.

WAXD

Wide-angle X-ray diffraction (WAXD) was measured by X-Ray Diffractometer on a D8 Advance, Bruker.

Stress-Strain

Polymers were melt-pressed at 10 to 30 °C above their respective melting point to fabricate the dog-bone-shaped tensile-test specimens, which were subsequently aged for 24 hours prior to mechanical testing. The test specimens showed 12 mm gauge length, 2 mm width, and thickness of 0.6 mm. Stress-strain experiments were performed at 50 m/min using a Universal Test Machine (KEZHUN, KZ-SSBC-500) at room temperature.

1.3 Computational Details of Steric Maps

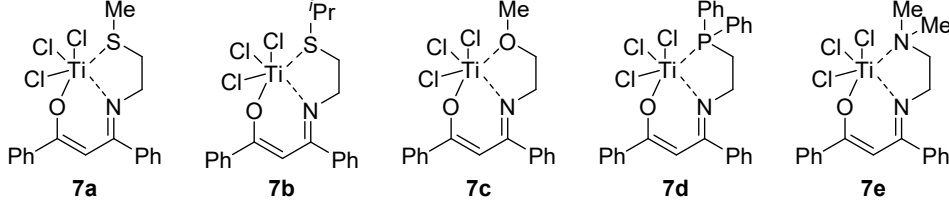
Corresponding DFT computations were carried out with the Gaussian 16 (Revision A.03) program.³ Geometry optimizations and frequency calculations were performed using the B3LYP density functional^{4,5} with Grimme's D3(BJ) dispersion.⁶ The 6-31G(d,p)⁷⁻⁹ basis set was adopted for all of the atoms. Frequency analysis was conducted at the same level of theory at 298.15K to confirm the stationary points as minima with zero imaginary frequencies. The steric map for analyzing catalytic pocket was built with SambVca 2.¹⁰

1.4 General Procedure of Polymerization of 1-Butene

After heat-drying a 50 mL sealed tube (equipped with a rubber stopper and magnetic stirrer) at 110 °C under vacuum and replacing the atmosphere with argon three times, connect the tube to a 1-butene gas supply. Once cooled to room temperature, place it in a low-temperature reactor set to -20 °C to condense liquid 1-butene. At this temperature, inject the alkylaluminum and titanium catalyst solution via syringe, stir for 5 min, and add the $[\text{Ph}_3\text{C}][\text{B}(\text{C}_6\text{F}_5)_4]$ solution (when using methylaluminoxane as co-catalyst, $[\text{Ph}_3\text{C}][\text{B}(\text{C}_6\text{F}_5)_4]$ did not need to be added, and the operation sequence was monomer-(M)MAO-catalysts). Seal with a PTFE plug and react at the specified temperature. After the required time, vent residual gas, pour the mixture into acidified ethanol to quench, stir thoroughly, filter, collect the polymer, and dry in a vacuum oven at 60 °C to constant weight.

2. Supplementary Table

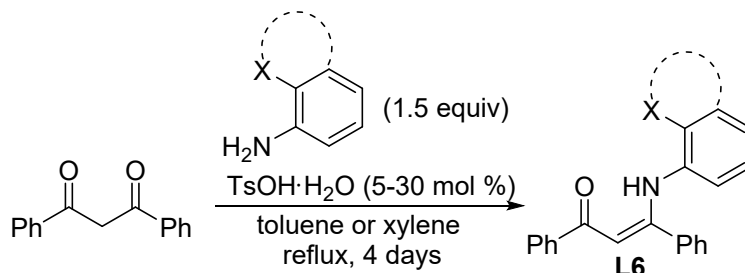
Table S1. Polymerization of 1-butene with reported tridentate [O-NX] titanium complexes.^a

							
Entry	Cat.	Co-cat.	Al/Ti/B	Solvent	Time (min)	Yield (g)	Act. ^b
1	7a	MMAO	500/1/0	toluene	120	0.73	0.37
2	7a	AlEt ₃ /[Ph ₃ C][B(C ₆ F ₅) ₄]	25/1/1	toluene	30	0.02	0.04
3	7a	AlEt ₃ /[Ph ₃ C][B(C ₆ F ₅) ₄]	25/1/1	DCM	30	n.p.	n.r.
4	7b	MMAO	500/1/0	toluene	120	0.73	0.37
5	7c	MMAO	500/1/0	toluene	120	0.08	0.04
6	7d	MMAO	500/1/0	toluene	120	0.92	0.46
7	7e	MMAO	500/1/0	toluene	120	n.p.	n.r.

^aReaction conditions: 1-butene (2.4–2.5 g), **7** (0.01 mmol in 2 mL toluene), co-catalyst, 25 °C, 30–120 min, in a sealed tube, quenched by acidified ethanol until the set time. ^bActivity is in unit of 10⁵ g·mol⁻¹·h⁻¹.

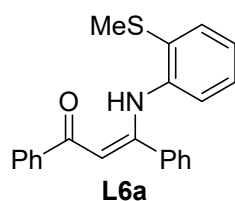
Initially, reported representative tridentate [O-NX] titanium complexes derived from 2-heteroatom substituted ethylamine, such as **7a–7e**, were tested in 1-butene polymerization because of their known performance in ethylene polymerization.¹¹ However, these reported complexes with side-arms bearing different heteroatoms all exhibited low activity, which may be due to the strong side-arm donors derived from alkylamines leading to lower Lewis acidity in the titanium center, resulting in weak coordination ability with monomers. Of note, alkylamine derived catalyst **7a** was not compatible with the alkyl aluminium/[Ph₃C][B(C₆F₅)₄] co-catalyst system (Table S1, entries 2, 3), while arylamine derived catalyst **6a** was exactly the opposite.

3. Synthesis and NMR Data of Ligands L6a–L6e.



General procedure for the synthesis of ligands (taking **L6a** as an example): To a solution of 1,3-diphenylpropane-1,3-dione (10.0 mmol, 2.24 g) and 2-(methylthio)aniline (15.0 mmol, 2.09 g) in toluene (50 mL) was added 4-methylbenzenesulfonic acid hydrate (0.5 mmol, 0.10 g) at room temperature. The flask was equipped with a water separator. The reaction mixture was heated to reflux for 4 days and the progress was monitored by TLC. Then, the solvent was removed under reduced pressure and the residue was purified by column chromatography on silica gel to give yellow solid **L6a** (6.0 mmol, 2.08 g, 60% yield). The ligands **L6b–L6d** were all synthesized as in the steps described above.

Synthesis of **L6e**: To a solution of 1,3-diphenylpropane-1,3-dione (10.0 mmol, 2.24 g) and 8-aminoquinoline (15.0 mmol, 2.16 g) in xylene (50 mL) was added 4-methylbenzenesulfonic acid hydrate (3 mmol, 0.57 g) at room temperature. The flask was equipped with a water separator. The reaction mixture was heated to reflux for 4 days and the progress was monitored by TLC. Then, the solvent was removed under reduced pressure and the residue was purified by column chromatography on silica gel to give yellow solid **L6e** (6.6 mmol, 2.31 g, 66% yield).

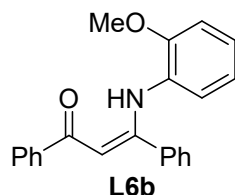


Synthesis of L6a: **L6a** was obtained in a yield of 60%.

¹H NMR (400 MHz, CDCl₃) δ 12.79 (s, 1H), 8.02 – 8.00 (m, 2H), 7.48 – 7.24 (m, 8H), 7.26 – 7.24 (m, 1H), 6.99 (td, *J* = 7.6, 1.2 Hz, 1H), 6.78 (td, *J* = 7.6, 1.2 Hz, 1H), 6.43 (d, *J* = 8.0 Hz, 1H), 6.17 (s, 1H), 2.54 (s, 3H).

¹³C NMR (100 MHz, CDCl₃) δ 189.8, 161.4, 139.8, 138.0, 136.0, 132.3, 131.3, 129.7, 128.5, 128.3, 128.2, 127.4, 127.1, 125.1(1), 125.0(7), 124.9, 97.6, 15.8.

ESI-MS Calcd for [C₂₂H₂₀NOS]⁺ (M + H⁺) 346.1260, found 346.1260.

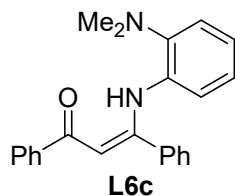


Synthesis of L6b: **L6b** was obtained in a yield of 73%.

¹H NMR (400 MHz, CDCl₃) δ 12.74 (s, 1H), 7.98 (d, *J* = 8.0 Hz, 2H), 7.48 – 7.31 (m, 8H), 6.94 (td, *J* = 8.0, 1.6 Hz, 1H), 6.85 (dd, *J* = 8.4, 1.2 Hz, 1H), 6.56 (td, *J* = 7.6, 1.2 Hz, 1H), 6.39 (d, *J* = 8.0 Hz, 1H), 6.09 (s, 1H), 3.90 (s, 3H).

¹³C NMR (100 MHz, CDCl₃) δ 189.4, 160.9, 151.2, 140.1, 136.3, 131.1, 129.5, 128.7, 128.4, 128.2, 128.0, 127.3, 124.5, 123.4, 119.9, 110.8, 97.4, 55.7.

ESI-MS Calcd for [C₂₂H₂₀NO₂]⁺ (M + H⁺) 330.1489, found 330.1490.

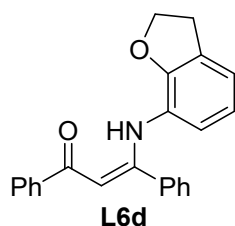


Synthesis of L6c: **L6c** was obtained in a yield of 81%.

¹H NMR (400 MHz, CDCl₃) δ 12.75 (s, 1H), 7.98 (dd, *J* = 8.0, 1.6 Hz, 2H), 7.48 – 7.33 (m, 8H), 7.01 (d, *J* = 8.0 Hz, 1H), 6.64 (td, *J* = 7.6, 1.6 Hz, 1H), 6.64 (td, *J* = 7.6, 1.6 Hz, 1H), 6.38 (dd, *J* = 8.0, 1.2 Hz, 1H), 6.09 (s, 1H), 2.83 (s, 6H).

¹³C NMR (100 MHz, CDCl₃) δ 189.3, 160.3, 146.0, 140.2, 136.5, 133.3, 131.1, 129.5, 128.5, 128.3, 127.8, 127.3, 124.3, 123.8, 122.0, 119.0, 97.2, 43.60.

ESI-MS Calcd for [C₂₃H₂₂N₂NaO]⁺ (M + Na⁺) 365.1624, found 365.1642.

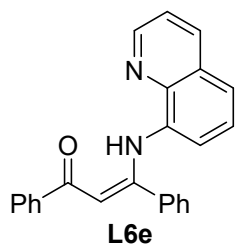


Synthesis of L6d: L6d was obtained in a yield of 90%.

¹H NMR (400 MHz, CDCl₃) δ 12.79 (s, 1H), 7.98 (dd, *J* = 8.0, 1.6 Hz, 2H), 7.47 – 7.33 (m, 8H), 6.84 (dd, *J* = 7.2, 1.2 Hz, 1H), 6.49 (t, *J* = 7.6 Hz, 1H), 6.24 (d, *J* = 8.0 Hz, 1H), 6.08 (s, 1H), 4.58 (t, *J* = 8.8 Hz, 2H), 3.20 (t, *J* = 8.8 Hz, 2H).

¹³C NMR (100 MHz, CDCl₃) δ 189.4, 161.3, 151.9, 139.9, 136.2, 131.1, 129.6, 128.4, 128.3, 128.1, 127.7, 127.3, 123.3, 121.8, 120.5, 120.1, 96.9, 71.7, 30.2.

ESI-MS Calcd for [C₂₃H₂₀NO₂]⁺ (M + H⁺) 342.1489, found 342.1452.



Synthesis of L6e: L6e was obtained in a yield of 66%.

¹H NMR (400 MHz, CDCl₃) δ 13.72 (s, 1H), 9.09 (dd, *J* = 4.0, 1.6 Hz, 1H), 8.12 (dd, *J* = 8.4, 1.6 Hz, 1H), 8.06 – 8.04 (m, 2H), 7.53 – 7.35 (m, 10H), 7.08 (t, *J* = 8.0 Hz, 1H), 6.49 (d, *J* = 7.6 Hz, 1H), 6.22 (s, 1H).

¹³C NMR (100 MHz, CDCl₃) δ 189.9, 158.9, 149.6, 140.6, 140.0, 136.6, 136.6, 136.0, 131.3, 129.7, 128.8, 128.6, 128.3, 128.1, 127.6, 125.9, 121.8, 121.5, 118.4, 99.9.

ESI-MS Calcd for [C₂₄H₁₈N₂NaO]⁺ (M + Na⁺) 373.1311, found 342.1316.

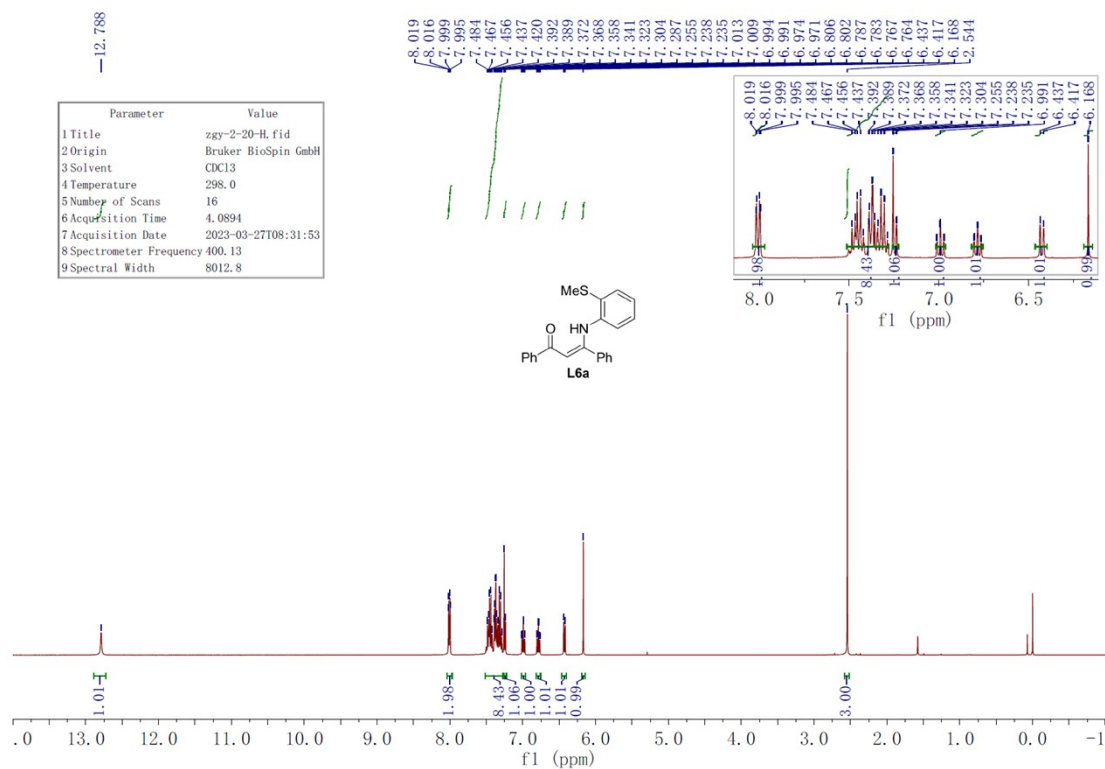


Figure S1. ^1H NMR spectrum (400 MHz, 298 K, CDCl_3) of L6a.

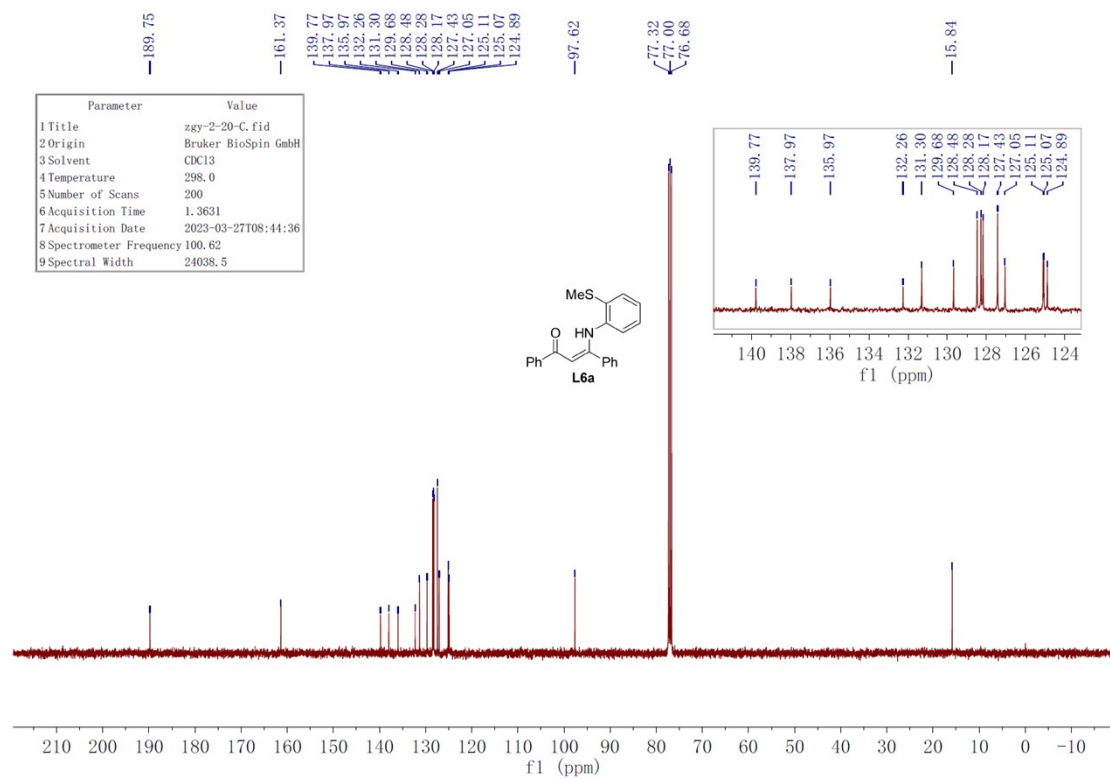


Figure S2. ^{13}C NMR spectrum (100 MHz, 298 K, CDCl_3) of L6a.

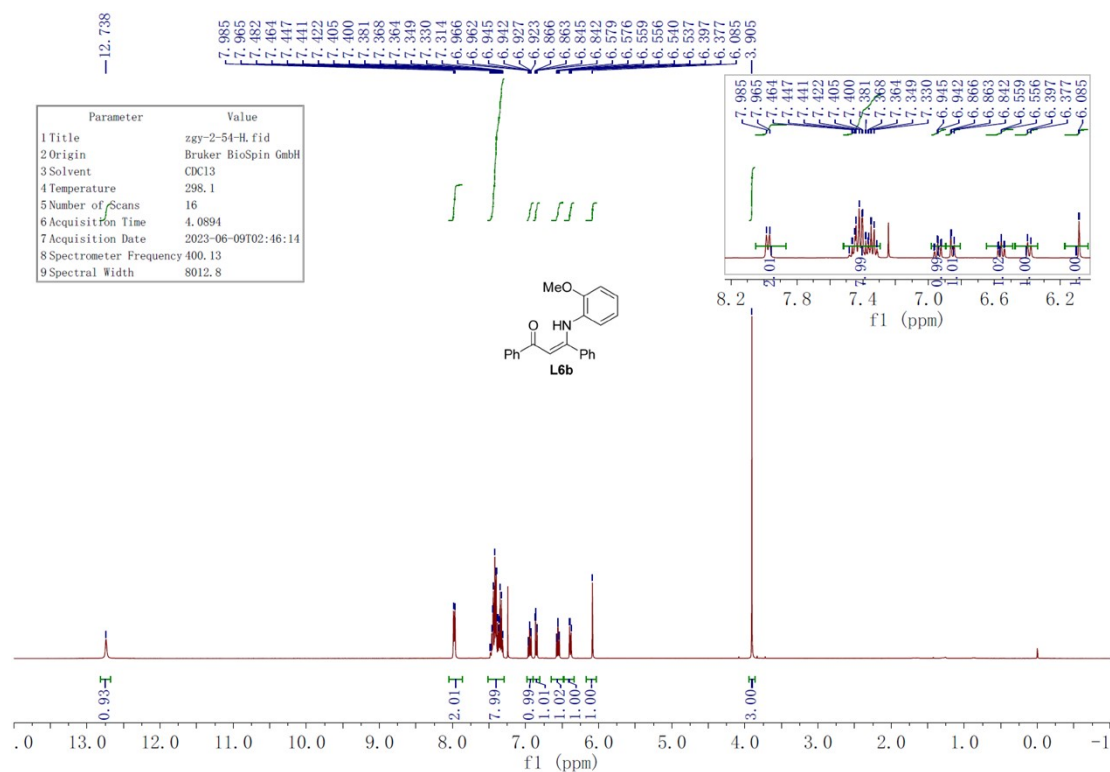


Figure S3. ^1H NMR spectrum (400 MHz, 298 K, CDCl_3) of **L6b**.

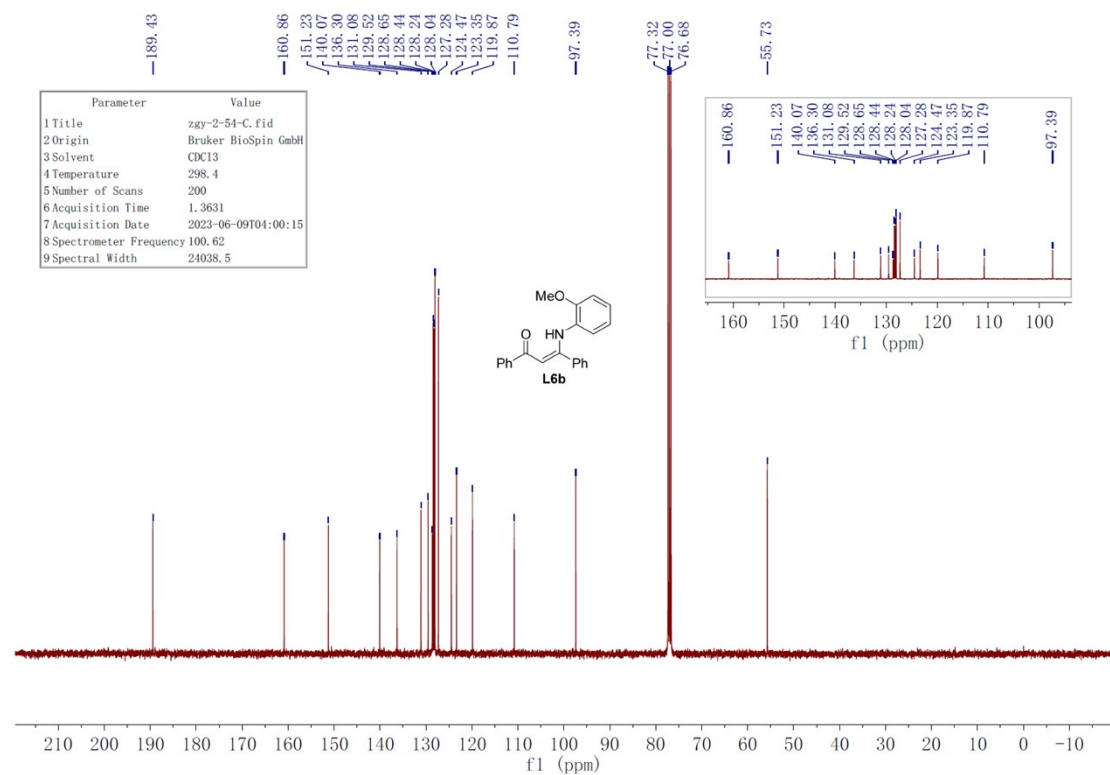


Figure S4. ^{13}C NMR spectrum (100 MHz, 298 K, CDCl_3) of **L6b**.

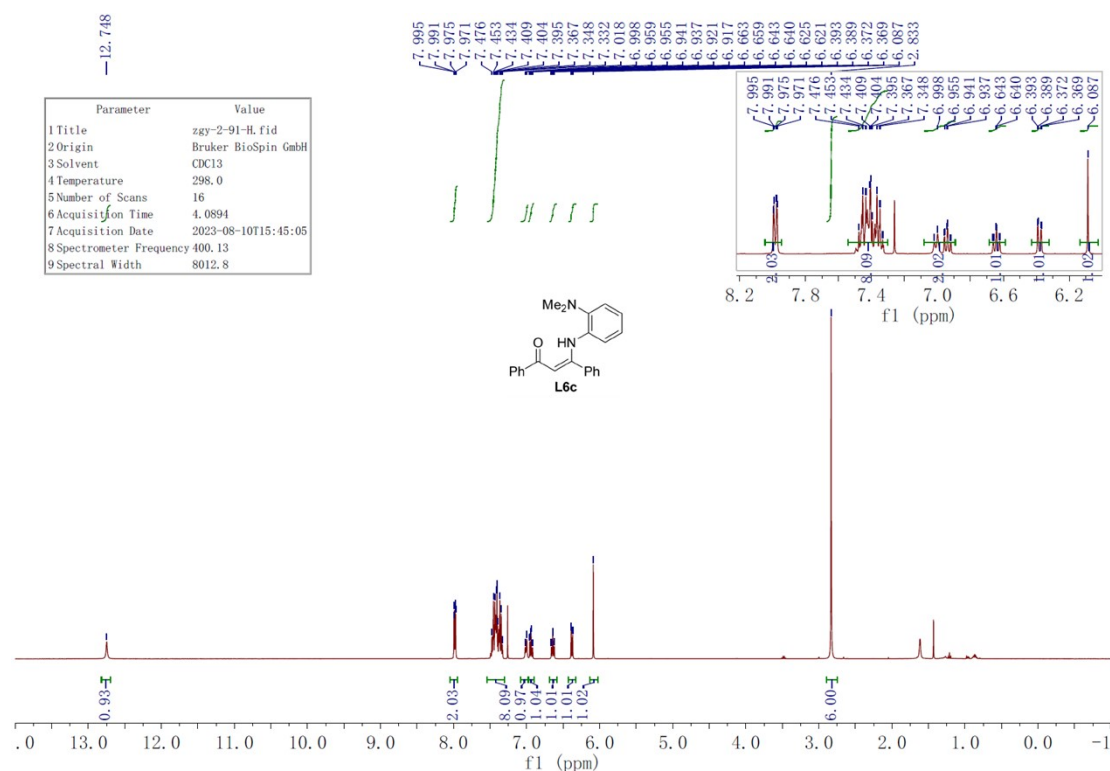


Figure S5. ¹H NMR spectrum (400 MHz, 298 K, CDCl₃) of L6c.

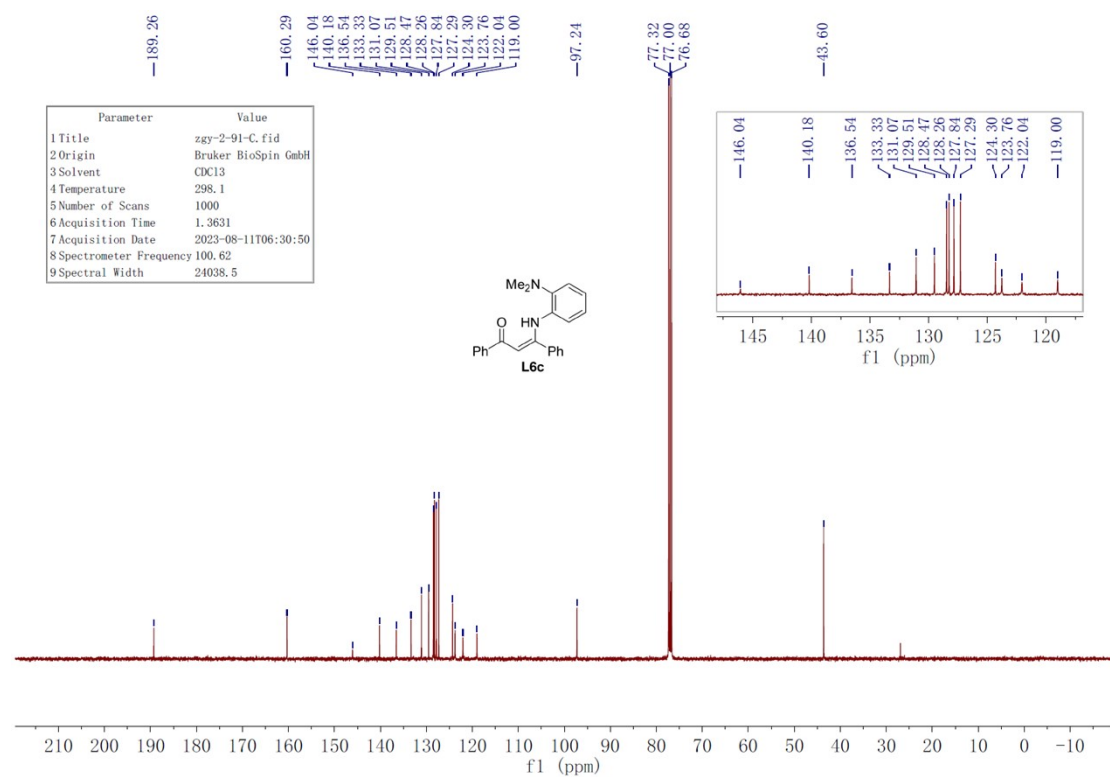


Figure S6. ¹³C NMR spectrum (100 MHz, 298 K, CDCl₃) of L6c.

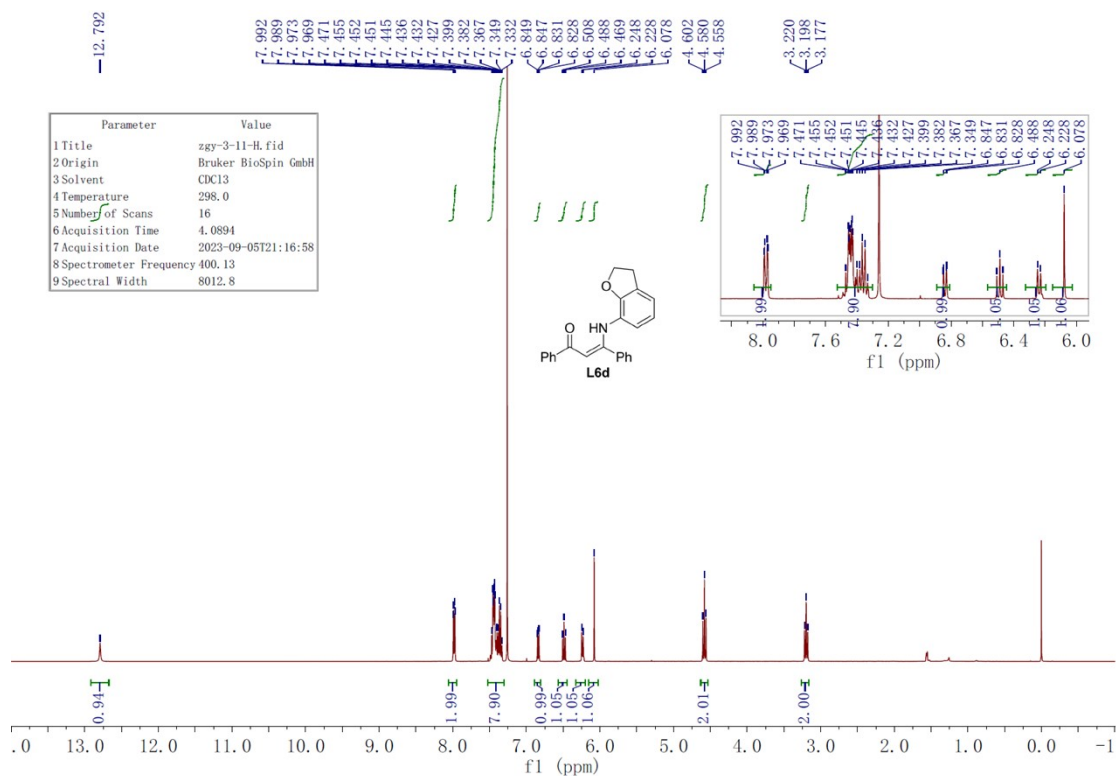


Figure S7. ¹H NMR spectrum (400 MHz, 298 K, CDCl₃) of L6d.

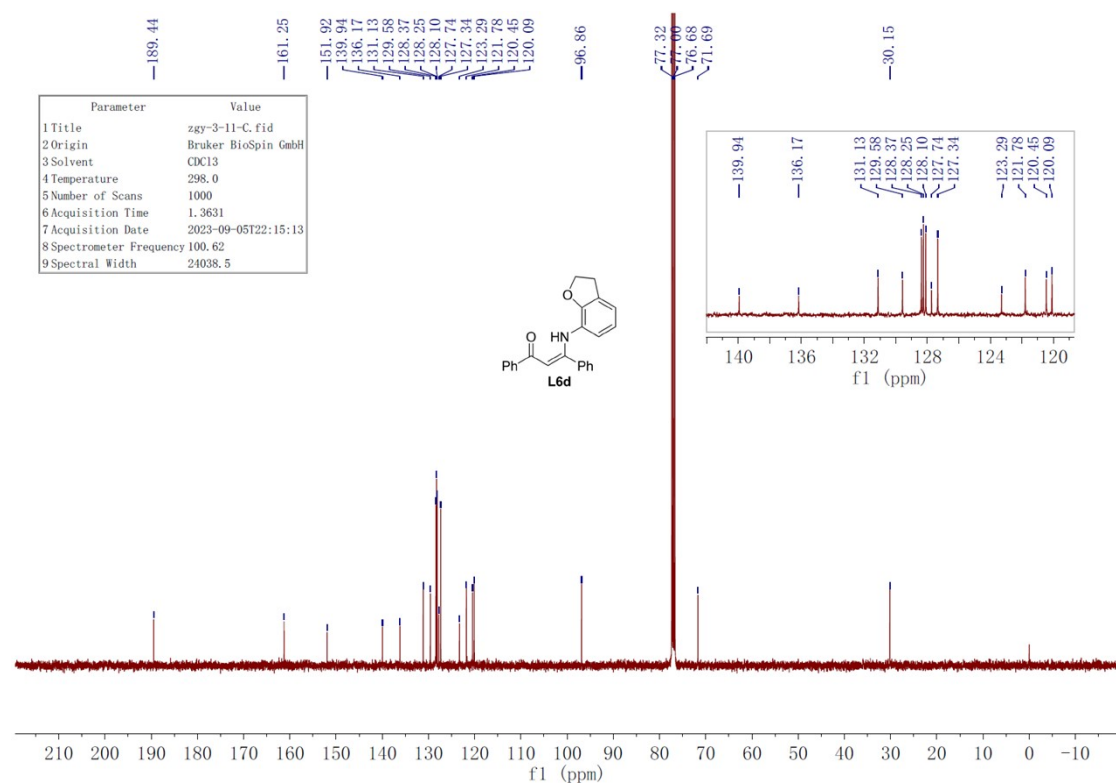


Figure S8. ¹³C NMR spectrum (100 MHz, 298 K, CDCl₃) of L6d.

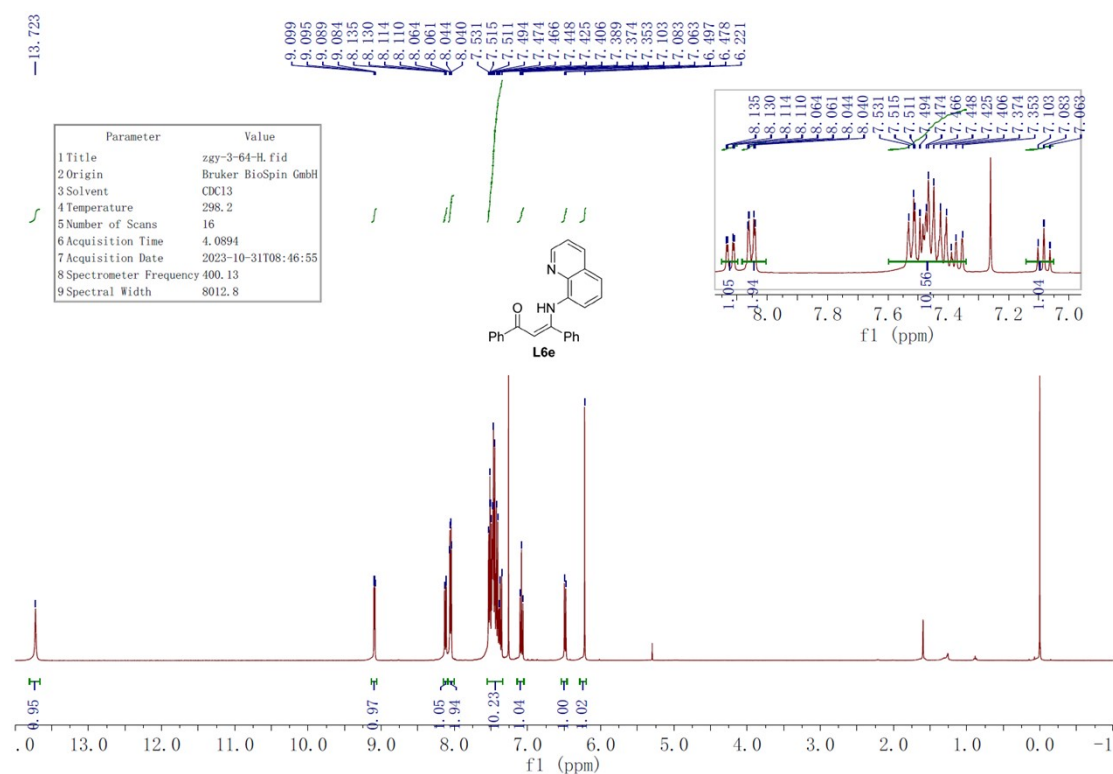


Figure S9. ¹H NMR spectrum (400 MHz, 298 K, CDCl₃) of **L6e**.

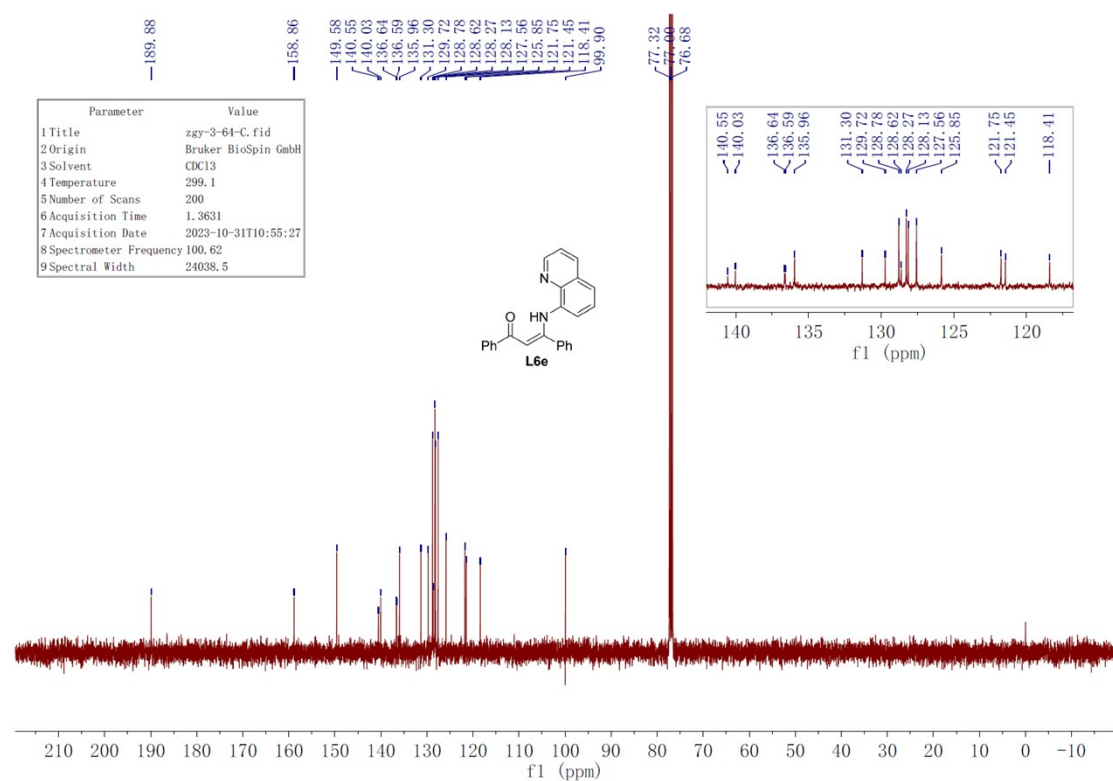
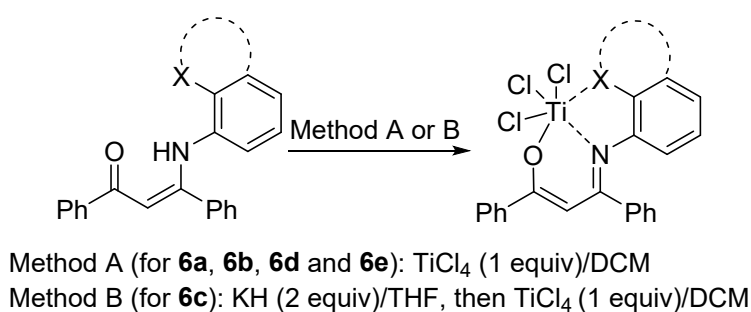


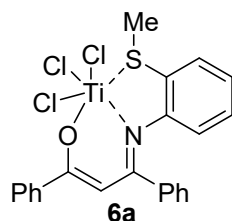
Figure S10. ¹³C NMR spectrum (100 MHz, 298 K, CDCl₃) of **L6e**.

4. Synthesis and NMR Data of Tridentate [O-NX] Titanium Complexes **6a–6e**.



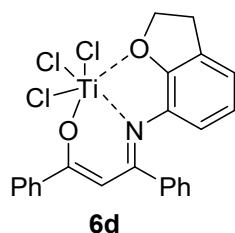
General procedure for the synthesis of **6a**, **6b**, **6d** and **6e** (Taking **6a** as an example, Method A): To a solution of ligand **L6a** (0.2 mmol, 69.1 mg) in dry DCM (5 mL) was added dropwise a solution of TiCl_4 (0.2 mmol, 37.9 mg) in dry DCM (1 mL) at room temperature. The solution was stirred for 3 h and filtered to remove the insoluble solid. The filtrate was concentrated under vacuum and added dropwise to 10 mL of hexane. The black solid precipitated from hexane was obtained and collected to yield complex **6a** (84.4 mg, 85%). Complexes **6b**, **6d** and **6e** were synthesized as above.

Synthesis of **6c** (Method B): To a suspension of potassium hydride (KH) (0.4 mmol, 16.0 mg) in dry THF (1 mL) was added a solution of **L6c** (0.2 mmol, 68.5 mg) in THF (5 mL) at -78°C . The resulting suspension was warmed to room temperature and stirred for 3 h. The solvent was removed under reduced pressure and the residue was dissolved in dry DCM (5 mL), and a solution of TiCl_4 (0.2 mmol, 37.9 mg) in dry DCM (1 mL) was added dropwise into above deprotonated ligand solution at room temperature. The solution was stirred for 12 h and filtered to remove the sylvite and other insoluble solid. The filtrate was concentrated under vacuum and then added dropwise to 10 mL of hexane. The black solid precipitated from hexane was obtained and collected to yield complex **6c** (67.9 mg, 69%).



Synthesis of 6a (Method A): **6a** was obtained in a yield of 85%.

Anal. calcd. for C₂₃H₂₁Cl₃N₂OTi: C 55.74; H 4.27. Found: C 55.94; H 4.53.

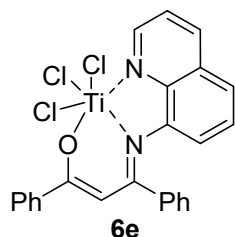


Synthesis of 6d (Method A): **6d** was obtained in a yield of 67%.

¹H NMR (400 MHz, CDCl₃) δ 7.87 – 7.85 (m, 2H), 7.55 – 7.41 (m, 8H), 6.96 (dd, *J* = 7.2, 0.8 Hz, 1H), 6.54 (t, *J* = 8.0 Hz, 1H), 6.43 (s, 1H), 5.81 (d, *J* = 8.4 Hz, 1H), 5.51 (t, *J* = 8.0 Hz, 2H), 3.45 (t, *J* = 8.0 Hz, 2H).

¹³C NMR (100 MHz, CDCl₃) δ 171.2, 169.0, 152.4, 137.6, 132.7, 131.4, 130.8, 130.0, 129.6, 129.1, 127.5, 127.1, 125.7, 124.5, 124.0, 120.8, 112.2, 81.5, 30.14.

Anal. calcd. for C₂₃H₁₈Cl₃NO₂Ti: C 55.85; H 3.67. Found: C 56.14; H 3.85.



Synthesis of 6e (Method A): **6e** was obtained in a yield of 76%.

¹H NMR (400 MHz, CDCl₃) δ 9.72 (dd, *J* = 4.8, 1.6 Hz, 1H), 8.43 (d, *J* = 8.4 Hz, 1H), 8.01 (d, *J* = 7.2 Hz, 2H), 7.72 (dd, *J* = 8.4, 4.8 Hz, 1H), 7.61 (d, *J* = 8.0 Hz, 1H), 7.56 (d, *J* = 7.2 Hz, 1H), 7.51 – 7.43 (m, 3H), 7.38 (t, *J* = 7.6 Hz, 2H), 7.31 – 7.30 (m, 2H), 7.18 (t, *J* = 8.0 Hz, 1H), 6.71 (s, 1H), 6.67 (d, *J* = 8.0 Hz, 1H).

¹³C NMR (100 MHz, CDCl₃) δ 173.1, 171.4, 151.6, 143.7, 142.4, 140.0, 138.3, 133.0, 132.1, 130.4, 129.4, 129.1, 128.0, 127.7, 127.3, 125.6, 124.4, 122.6, 112.2.

Anal. calcd. for C₂₄H₁₇Cl₃N₂OTi·1.5 CH₂Cl₂ (1.5 equiv. DCM in the tested sample): C 48.54; H 3.19. Found: C 48.11; H 3.05.

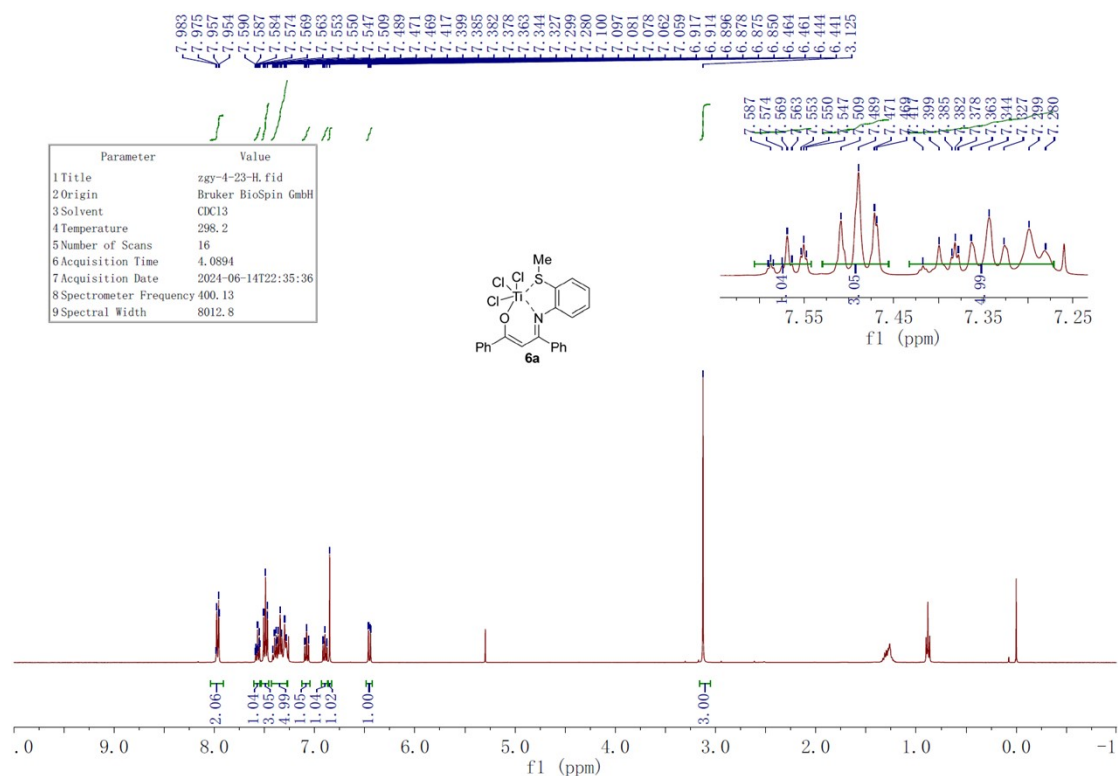


Figure S11. ¹H NMR spectrum (400 MHz, 298 K, CDCl₃) of **6a**.

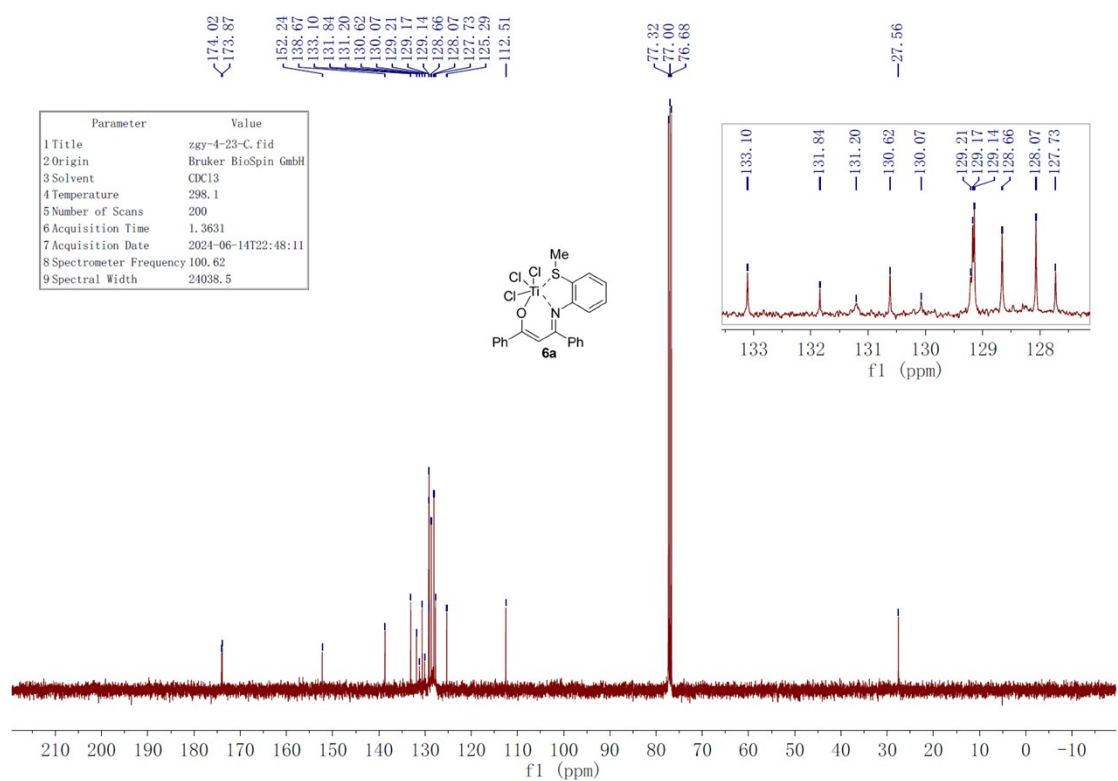


Figure S12. ¹³C NMR spectrum (100 MHz, 298 K, CDCl₃) of **6a**.

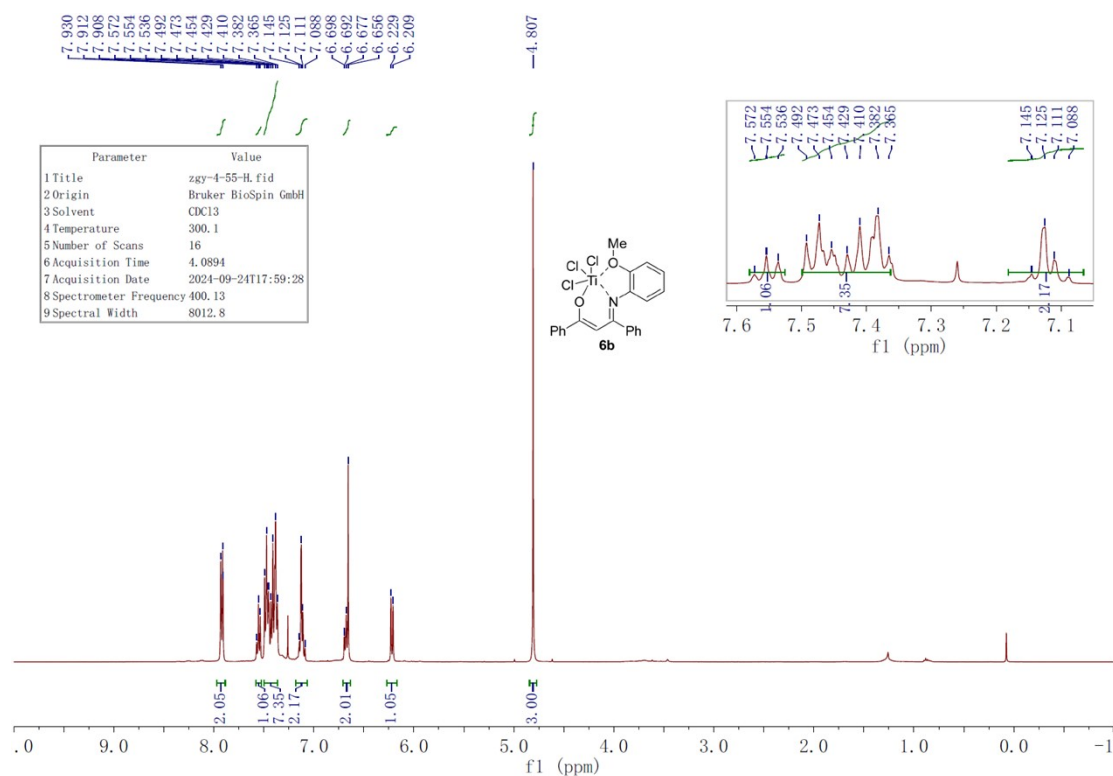


Figure S13. ^1H NMR spectrum (400 MHz, 298 K, CDCl_3) of **6b**.

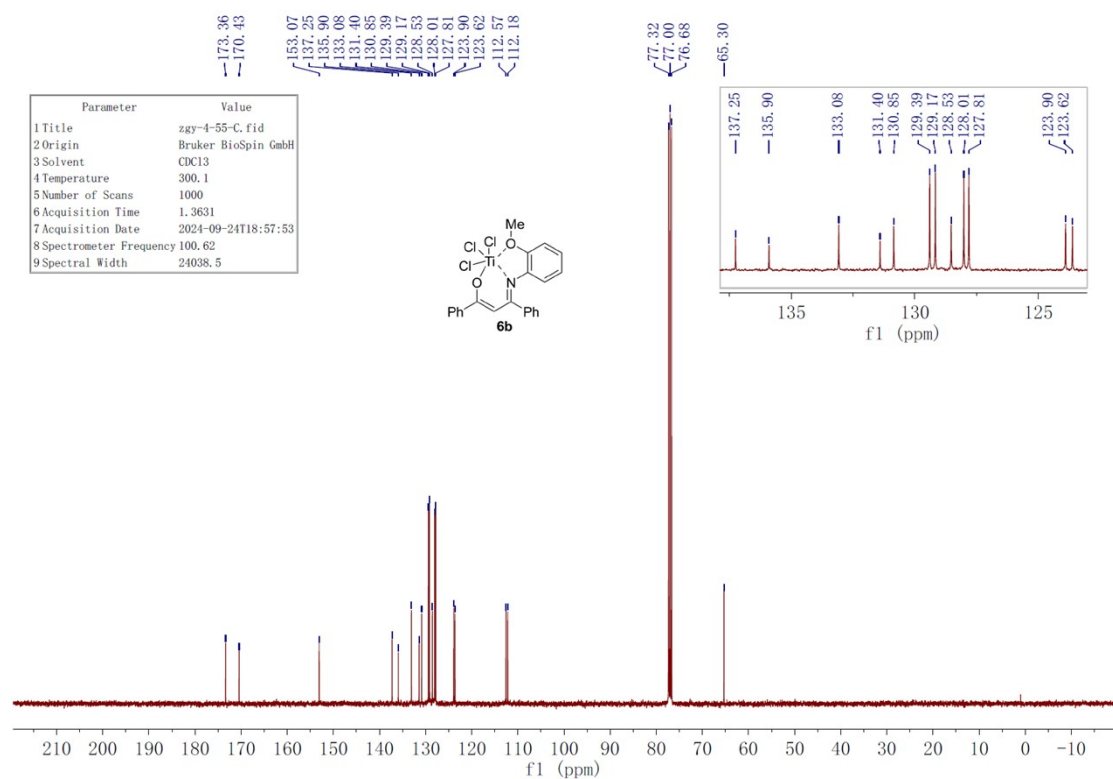


Figure S14. ^{13}C NMR spectrum (100 MHz, 298 K, CDCl_3) of **6b**.

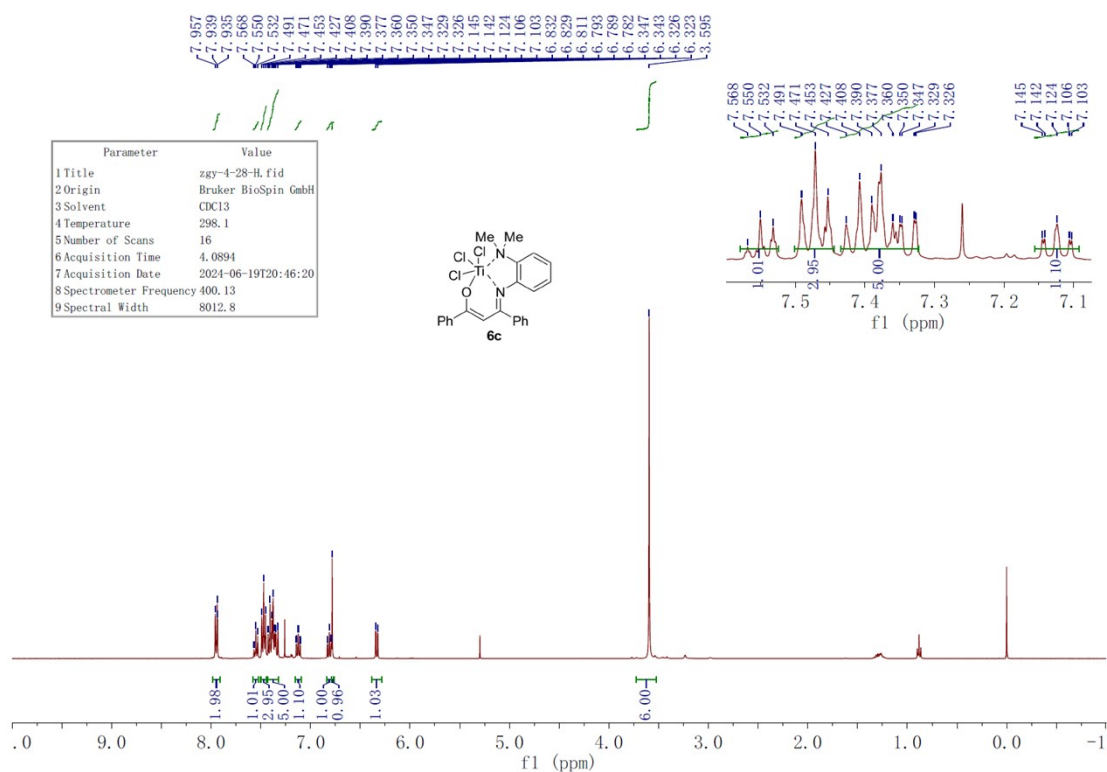


Figure S15. ^1H NMR spectrum (400 MHz, 298 K, CDCl_3) of **6c**.

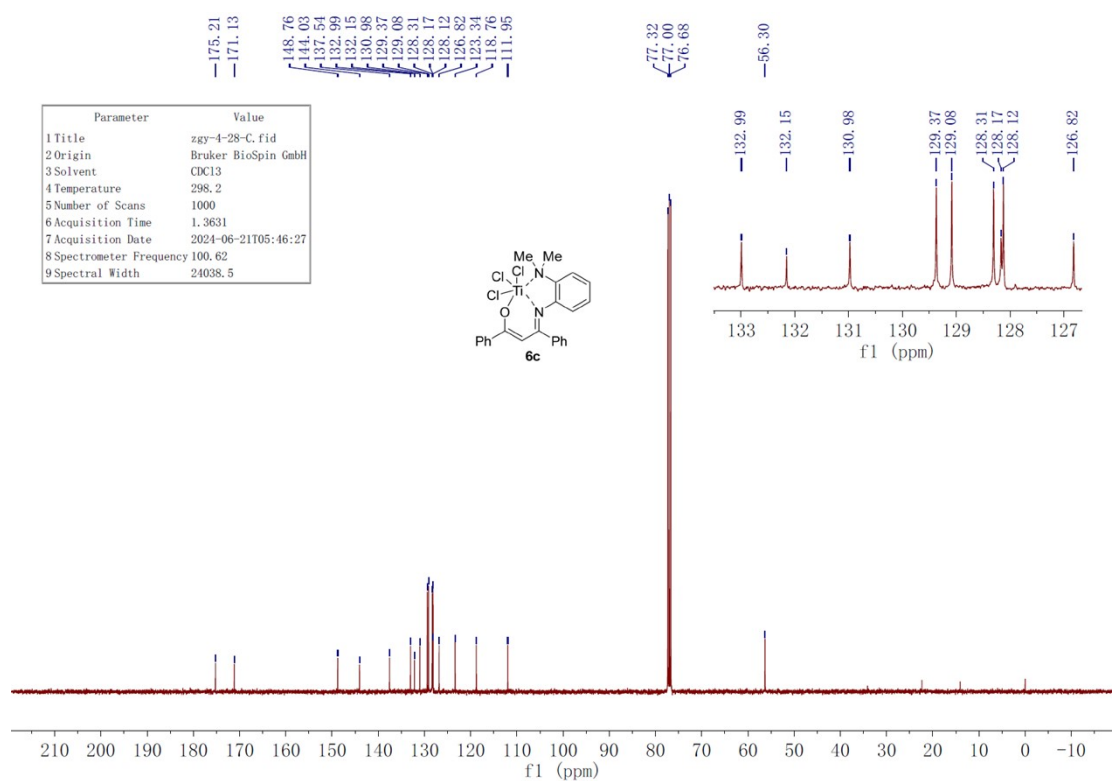


Figure S16. ^{13}C NMR spectrum (100 MHz, 298 K, CDCl_3) of **6c**.

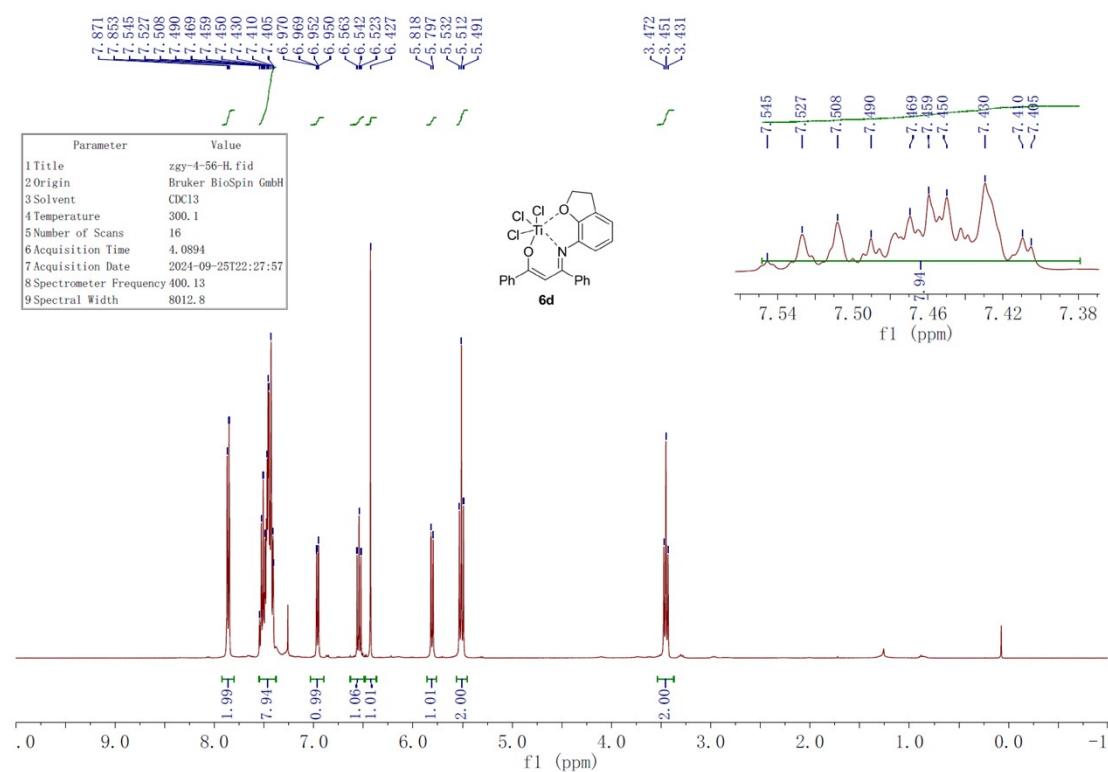


Figure S17. ^1H NMR spectrum (400 MHz, 298 K, CDCl_3) of **6d**.

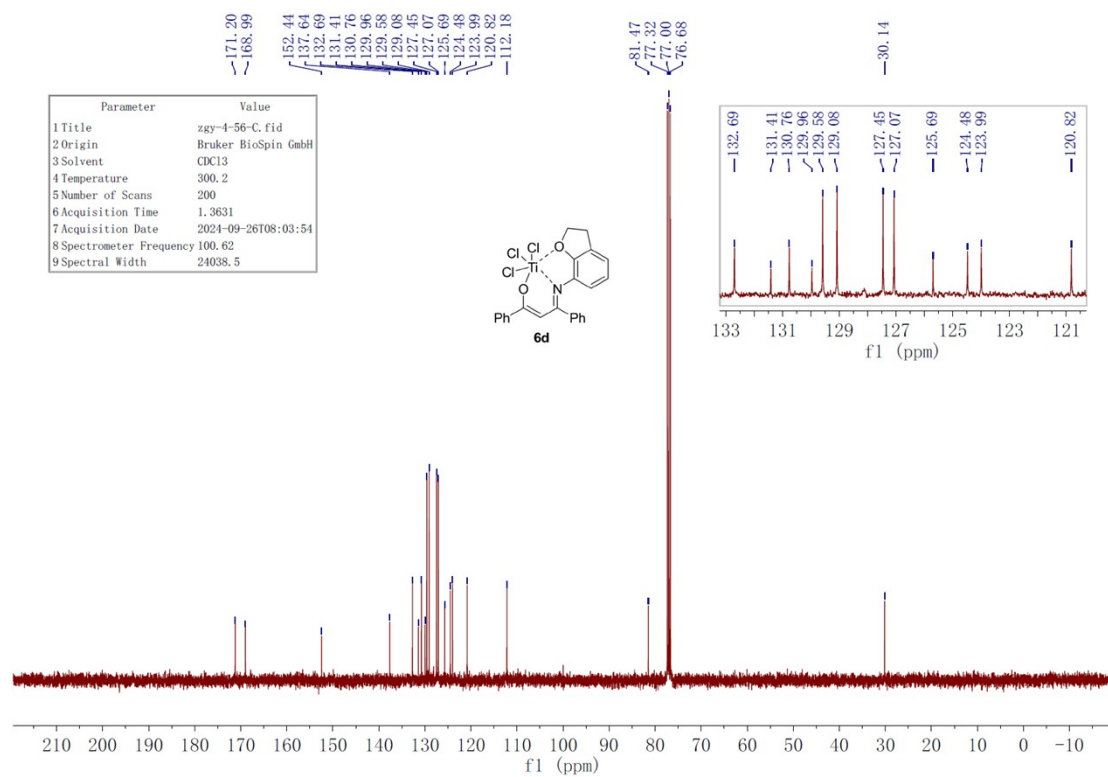


Figure S18. ^{13}C NMR spectrum (100 MHz, 298 K, CDCl_3) of **6d**.

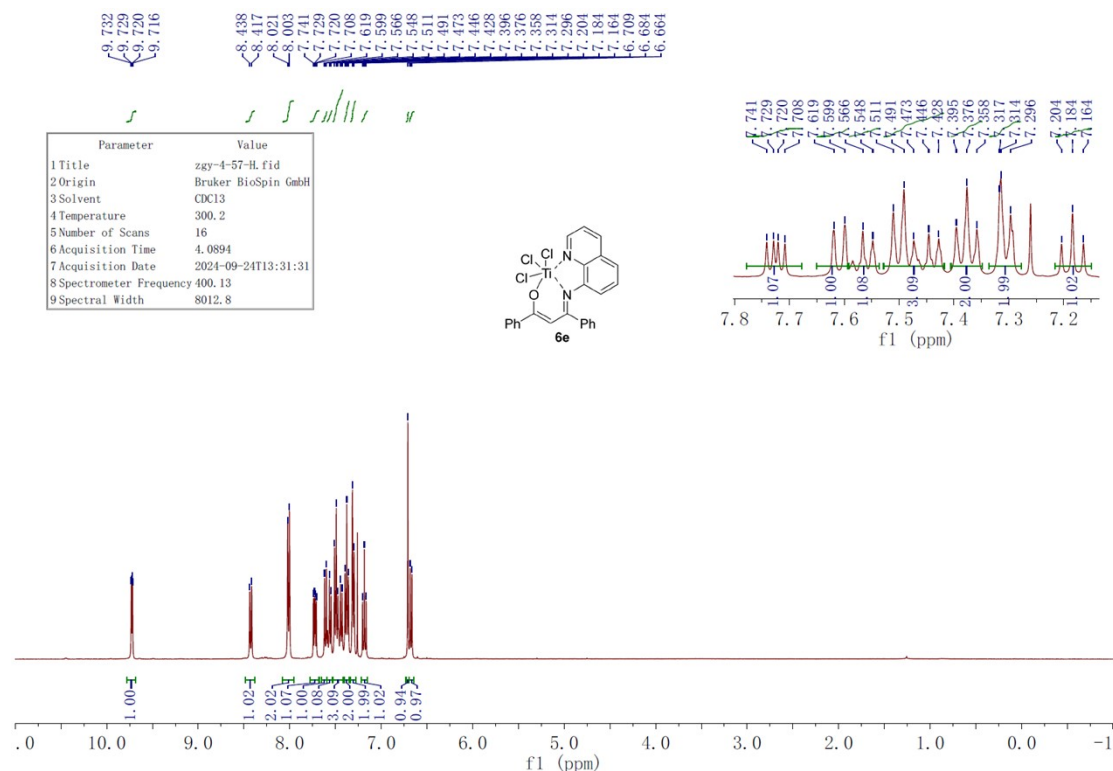


Figure S19. ¹H NMR spectrum (400 MHz, 298 K, CDCl₃) of **6e**.

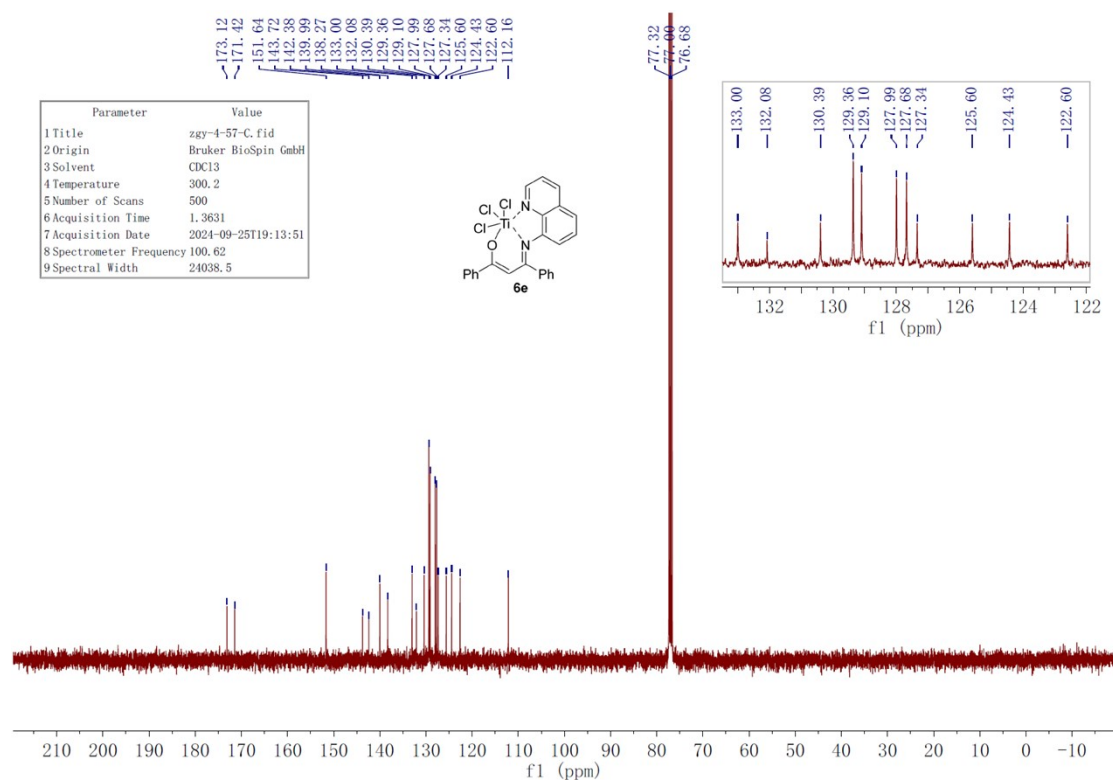


Figure S20. ¹³C NMR spectrum (100 MHz, 298 K, CDCl₃) of **6e**.

5. NMR Spectra of Polymers

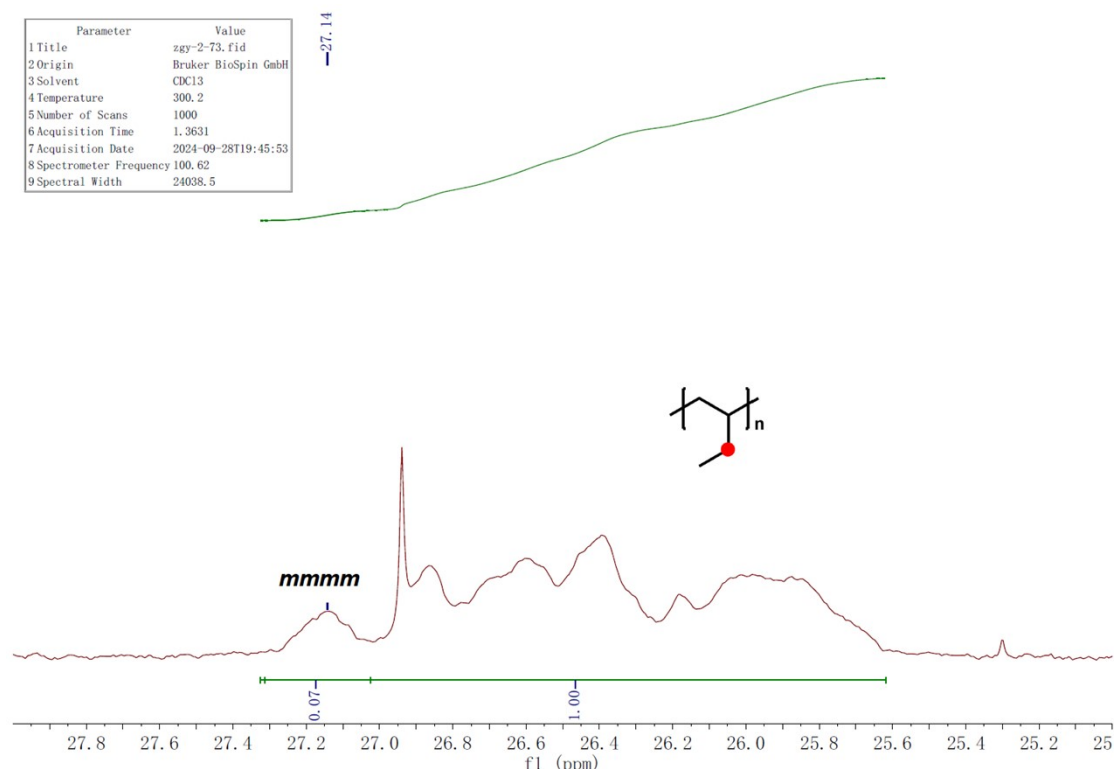


Figure S21. Quantitative ¹³C NMR spectrum (100 MHz, CDCl₃, 298 K) of the poly(1-butene) generated by complex **6a** from Table 1, Entry 10 or Table 2, Entry 1.

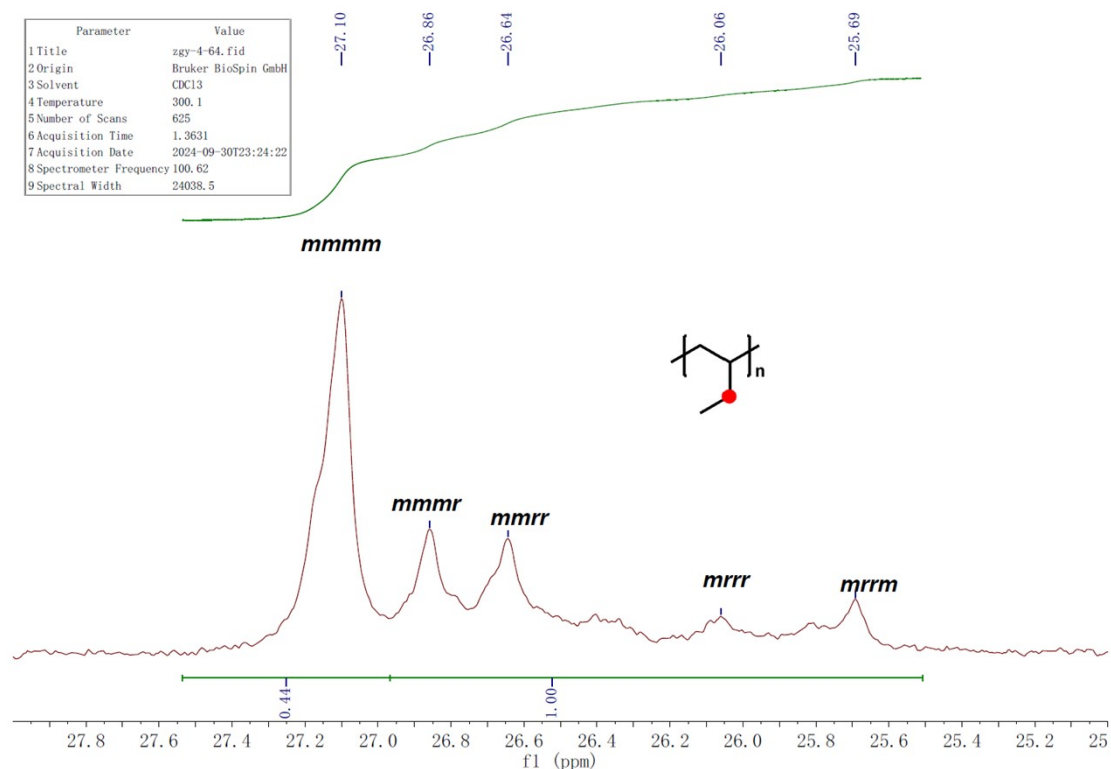


Figure S22. Quantitative ¹³C NMR spectrum (100 MHz, CDCl₃, 298 K) of the poly(1-butene) generated by complex **6b** from Table 2, Entry 2.

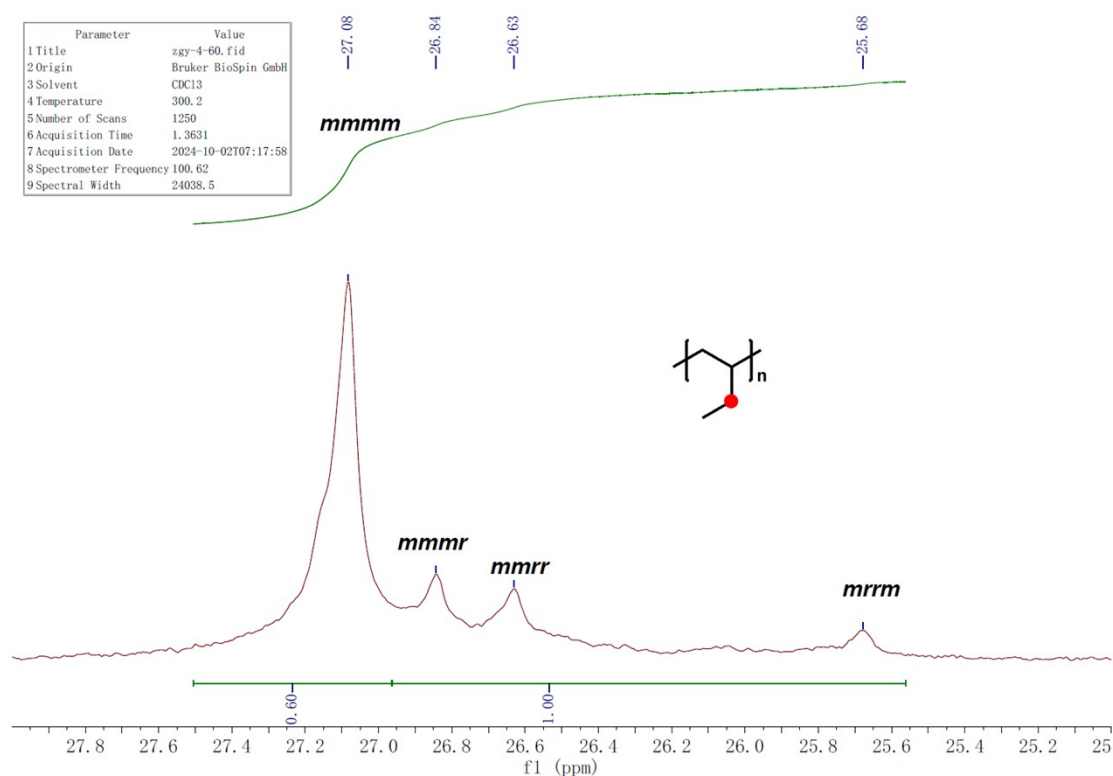


Figure S23. Quantitative ^{13}C NMR spectrum (100 MHz, CDCl_3 , 298 K) of the poly(1-butene) generated by complex **6d** from Table 2, Entry 5.

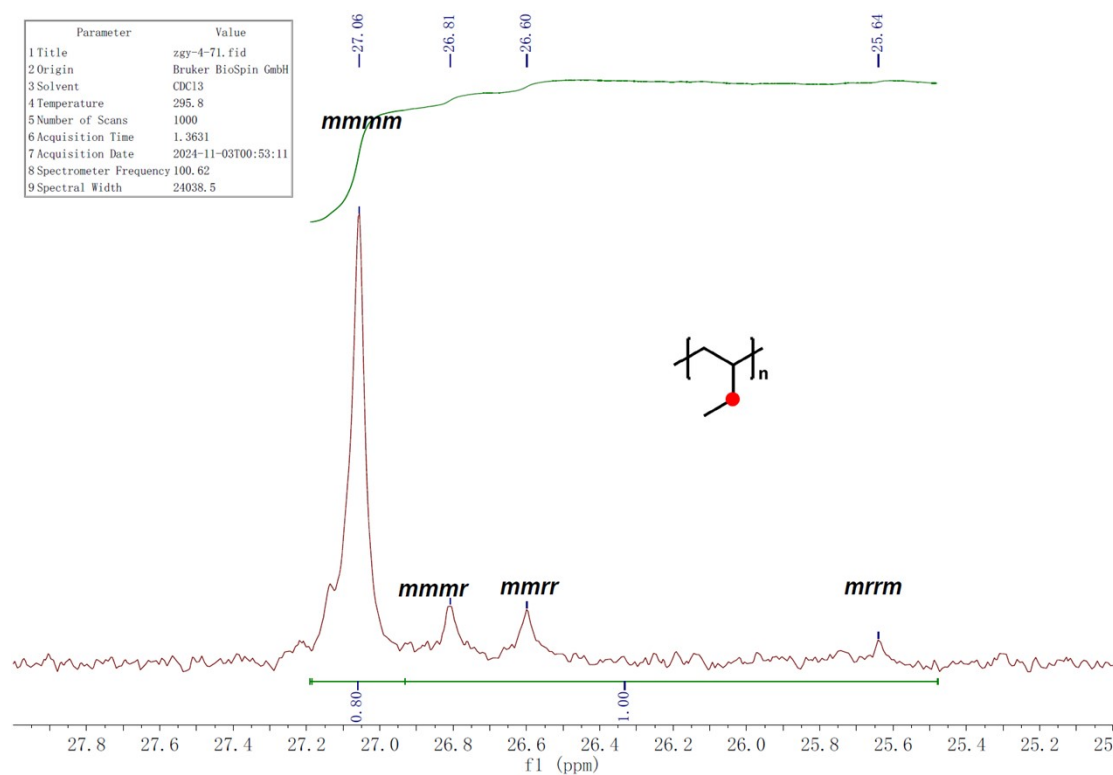


Figure S24. Quantitative ^{13}C NMR spectrum (100 MHz, CDCl_3 , 298 K) of the poly(1-butene) generated by complex **6d** from Table 2, Entry 6.

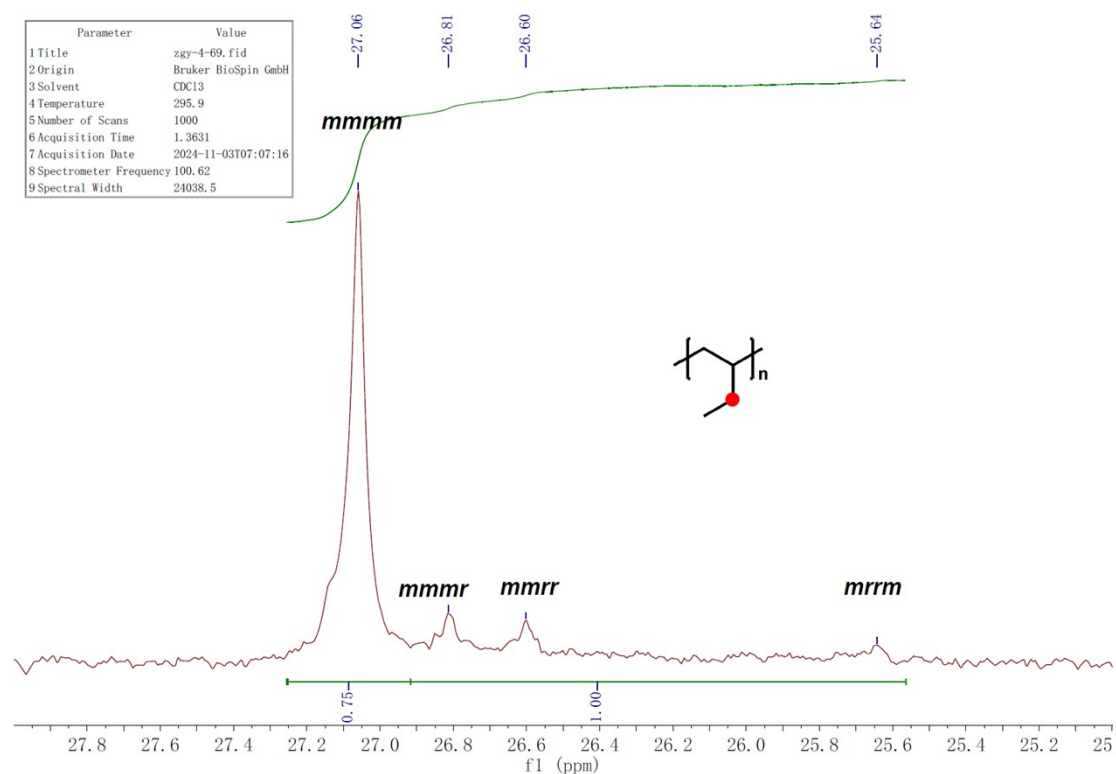


Figure S25. Quantitative ^{13}C NMR spectrum (100 MHz, CDCl_3 , 298 K) of the poly(1-butene) generated by complex **6d** from Table 2, Entry 7.

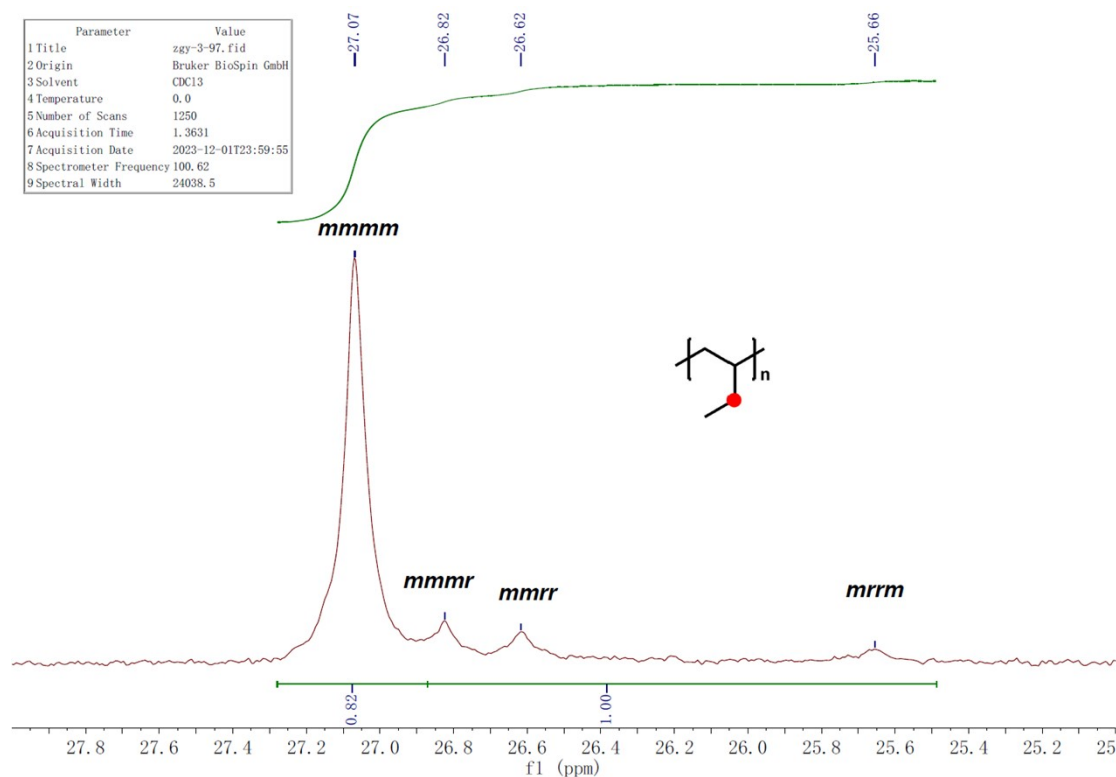


Figure S26. Quantitative ^{13}C NMR spectrum (100 MHz, CDCl_3 , 298 K) of the poly(1-butene) generated by complex **6e** from Table 2, Entry 8.

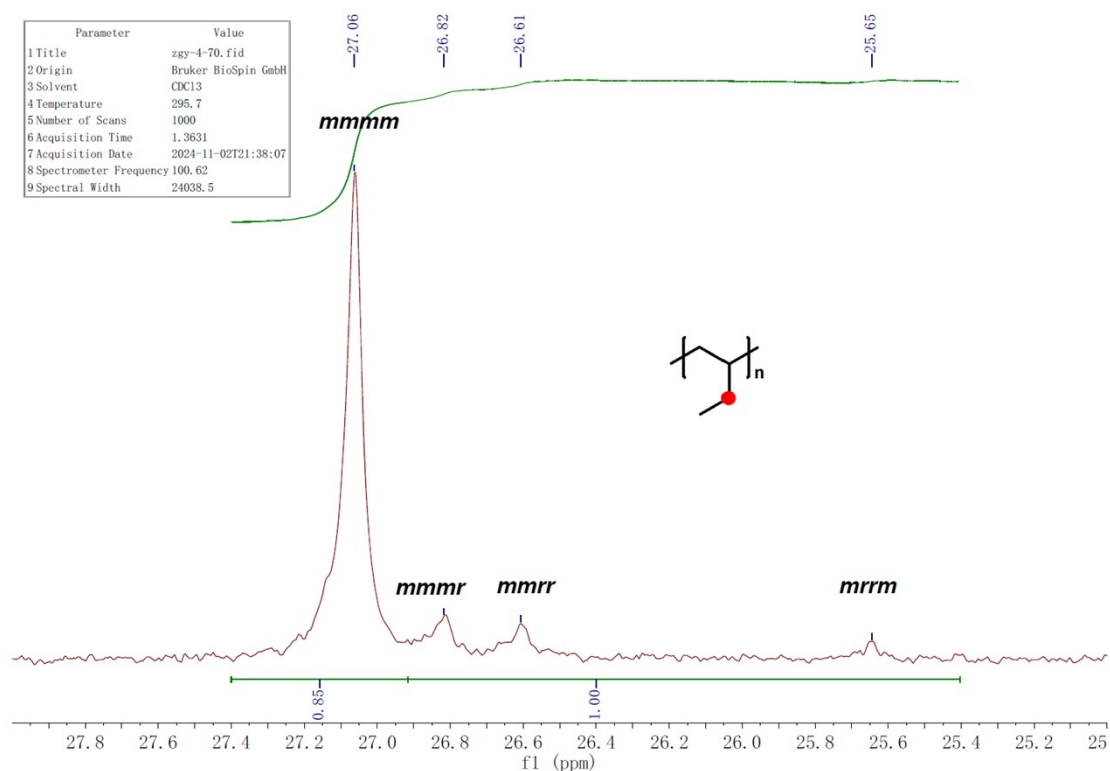


Figure S27. Quantitative ^{13}C NMR spectrum (100 MHz, CDCl_3 , 298 K) of the poly(1-butene) generated by complex **6e** from Table 2, Entry 9.

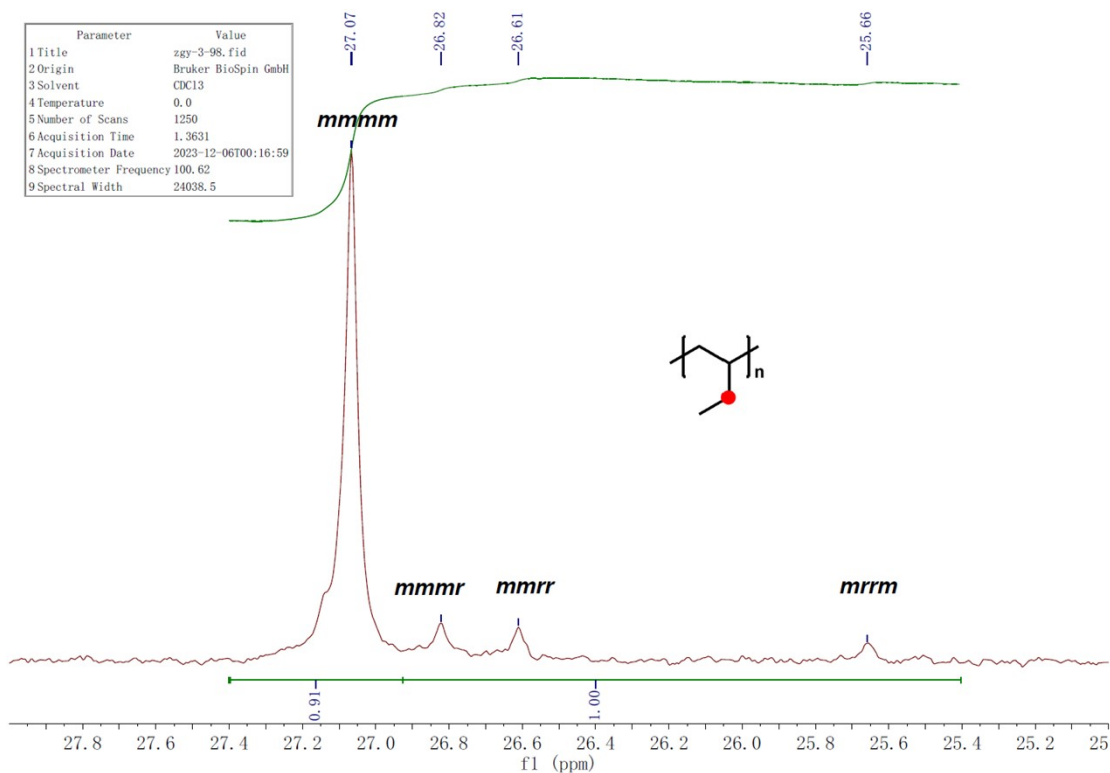
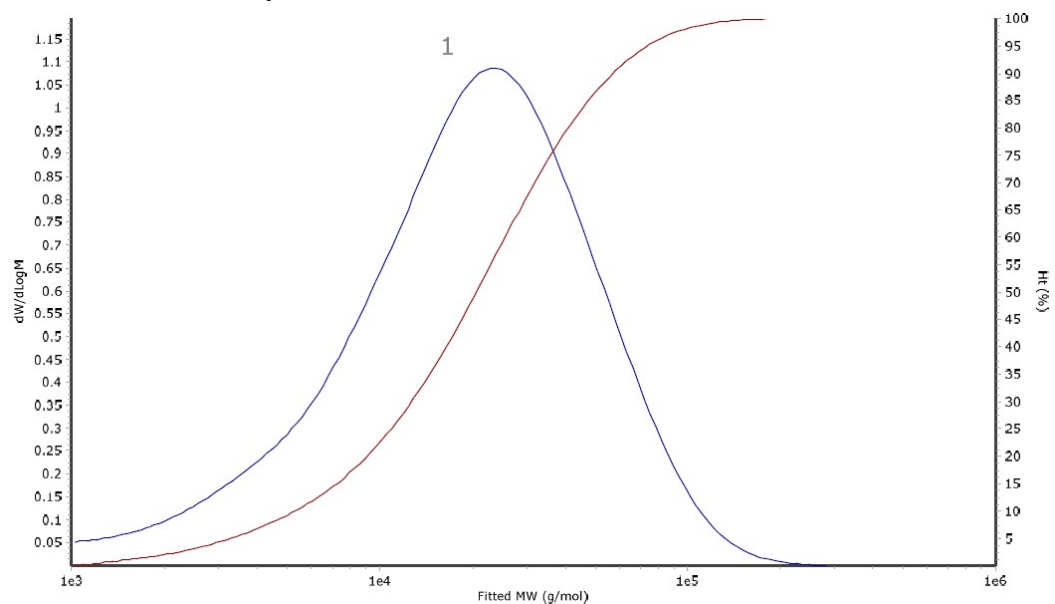


Figure S28. Quantitative ^{13}C NMR spectrum (100 MHz, CDCl_3 , 298 K) of the poly(1-butene) generated by complex **6e** from Table 2, Entry 10.

6. GPC Traces of Polymers



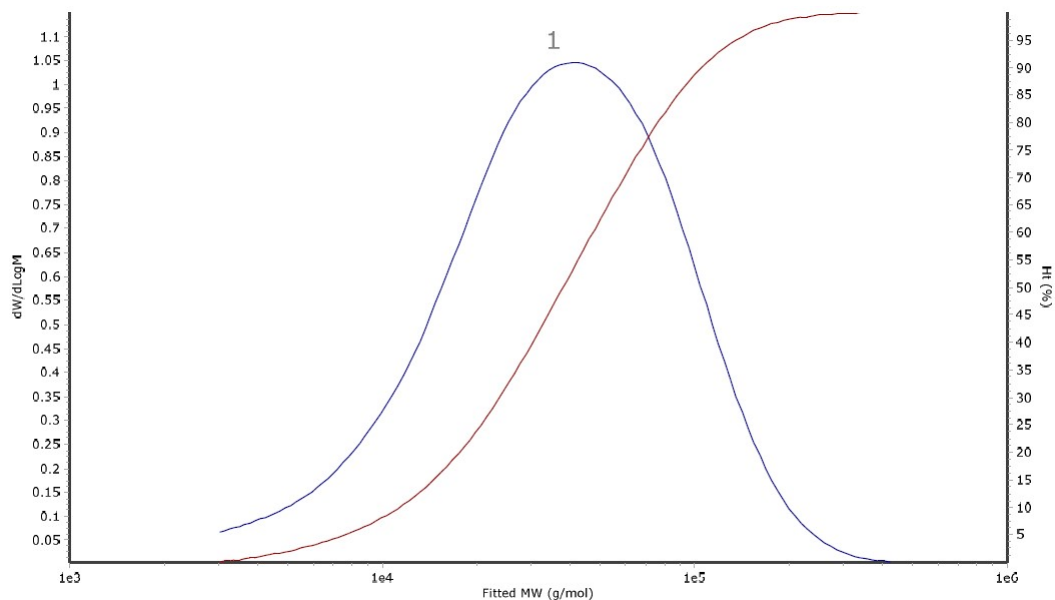
Molecular Weight Averages

Peak	Mp (g/mol)	Mn (g/mol)	Mw (g/mol)	Mz (g/mol)	Mz+1 (g/mol)	Mv (g/mol)	PD
Peak 1	23934	11483	27243	48200	72798	44948	2.372

Peak Trace Information

Peak	Trace	Peak Max RT (mins)	Peak Area (mV.s)	Peak Height (mV)
Peak 1	RI	8.07500	351548.910	6929.555

Figure S29. GPC trace of the poly(1-butene) (Table 1, Entry 1).



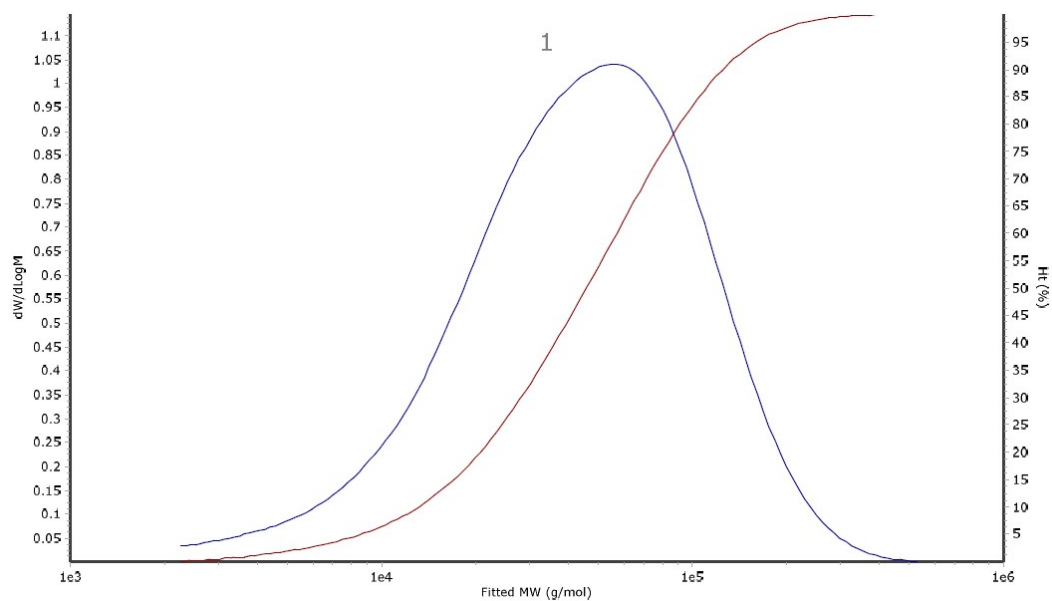
Molecular Weight Averages

Peak	Mp (g/mol)	Mn (g/mol)	Mw (g/mol)	Mz (g/mol)	Mz+1 (g/mol)	Mv (g/mol)	PD
Peak 1	42306	24202	50672	88447	133780	82468	2.094

Peak Trace Information

Peak	Trace	Peak Max RT (mins)	Peak Area (mV.s)	Peak Height (mV)
Peak 1	RI	7.85833	378197.804	7308.349

Figure S30. GPC trace of the poly(1-butene) (Table 1, Entry 2).



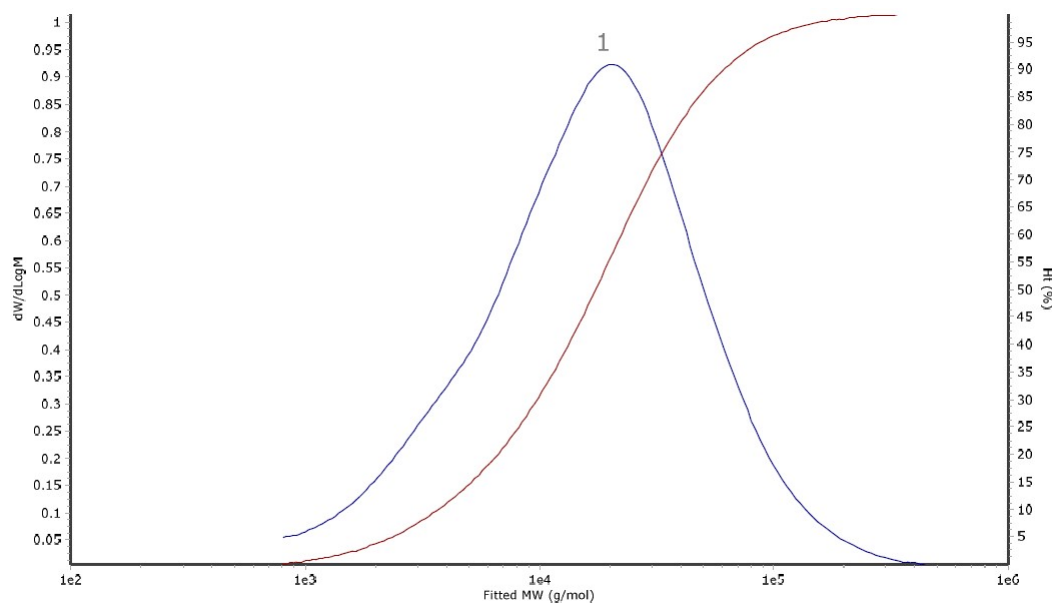
Molecular Weight Averages

Peak	Mp (g/mol)	Mn (g/mol)	Mw (g/mol)	Mz (g/mol)	Mz+1 (g/mol)	Mv (g/mol)	PD
Peak 1	57070	27147	60277	104590	156117	97723	2.22

Peak Trace Information

Peak	Trace	Peak Max RT (mins)	Peak Area (mV.s)	Peak Height (mV)
Peak 1	RI	7.74167	750497.712	14548.597

Figure S31. GPC trace of the poly(1-butene) (Table 1, Entry 3).



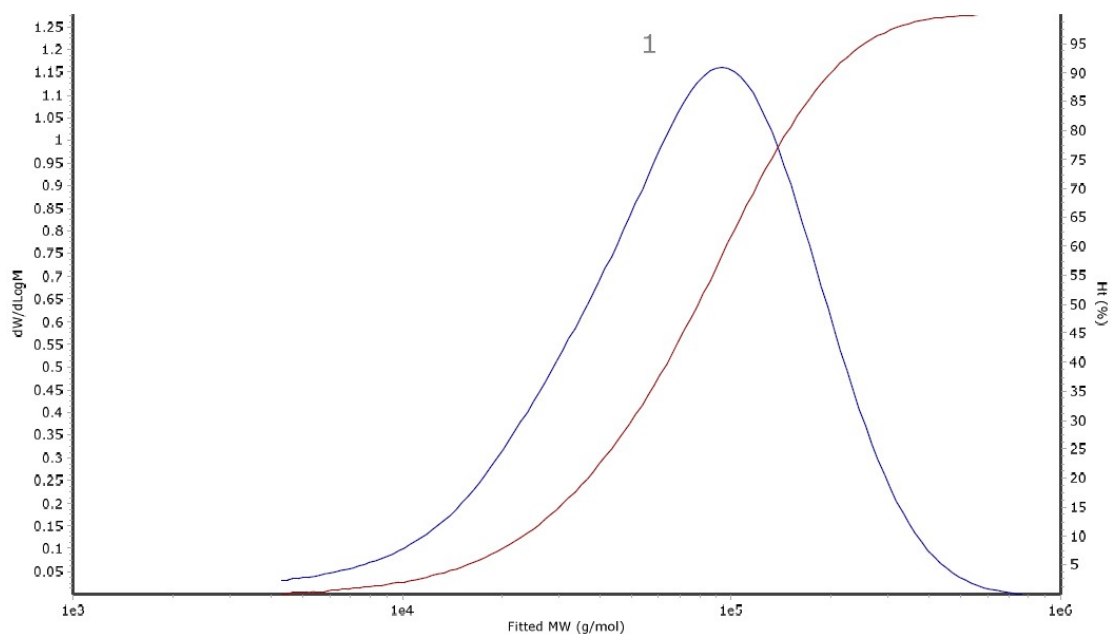
Molecular Weight Averages

Peak	Mp (g/mol)	Mn (g/mol)	Mw (g/mol)	Mz (g/mol)	Mz+1 (g/mol)	Mv (g/mol)	PD
Peak 1	20688	8832	27904	71935	146198	63494	3.159

Peak Trace Information

Peak	Trace	Peak Max RT (mins)	Peak Area (mV.s)	Peak Height (mV)
Peak 1	RI	8.13333	560476.615	9329.281

Figure S32. GPC trace of the poly(1-butene) (Table 1, Entry 4).



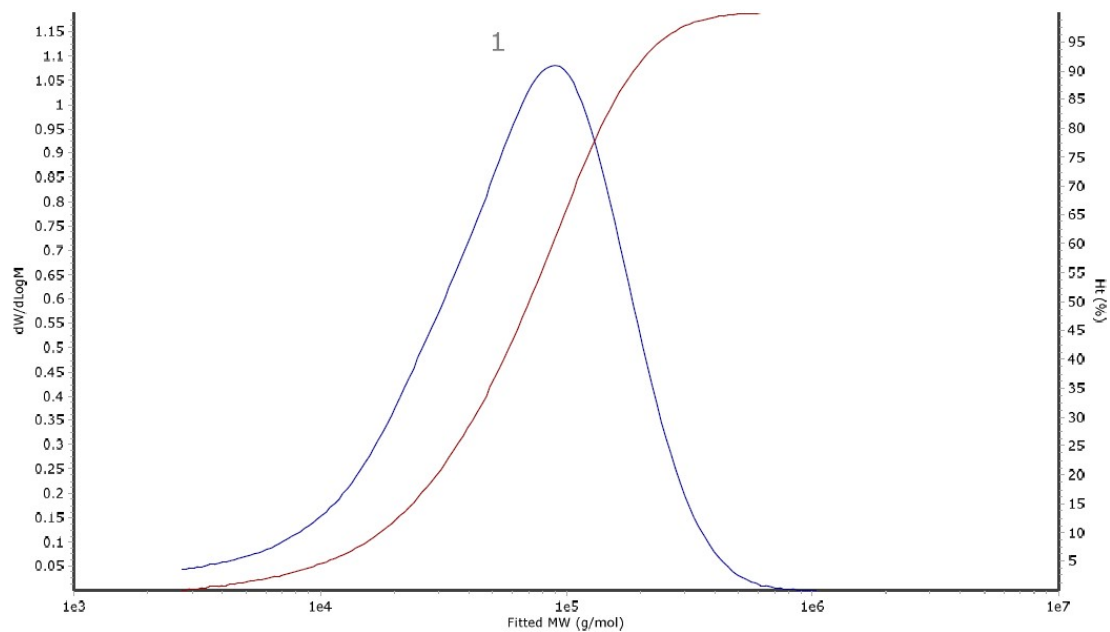
Molecular Weight Averages

Peak	Mp (g/mol)	Mn (g/mol)	Mw (g/mol)	Mz (g/mol)	Mz+1 (g/mol)	Mv (g/mol)	PD
Peak 1	93749	48515	99528	162985	233765	153353	2.051

Peak Trace Information

Peak	Trace	Peak Max RT (mins)	Peak Area (mV.s)	Peak Height (mV)
Peak 1	RI	7.54167	353117.368	7723.577

Figure S33. GPC trace of the poly(1-butene) (Table 1, Entry 5).



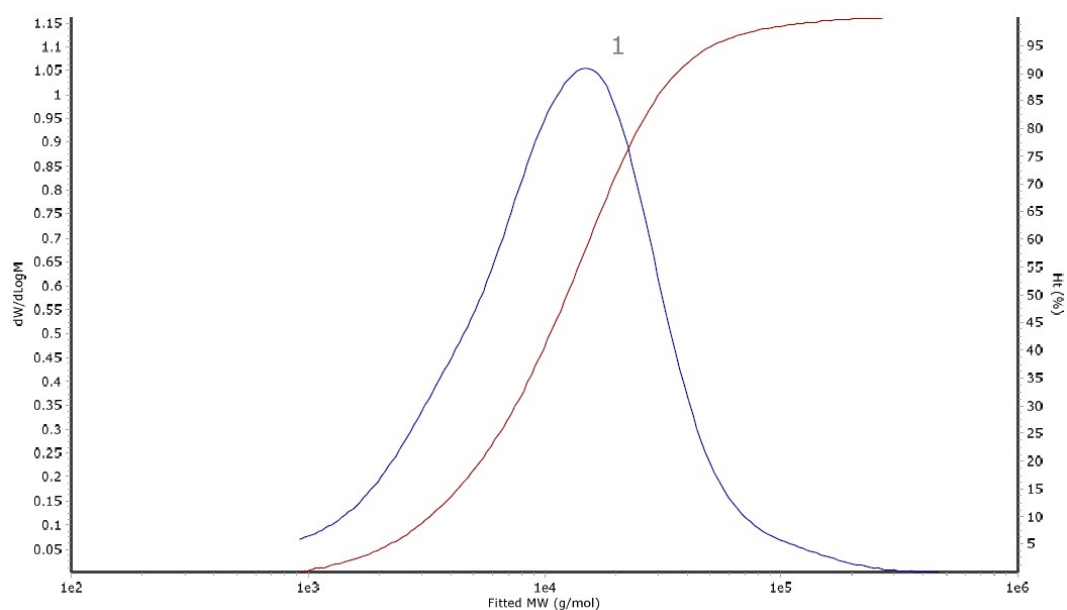
Molecular Weight Averages

Peak	Mp (g/mol)	Mn (g/mol)	Mw (g/mol)	Mz (g/mol)	Mz+1 (g/mol)	Mv (g/mol)	PD
Peak 1	89772	36926	91137	159272	240239	148804	2.468

Peak Trace Information

Peak	Trace	Peak Max RT (mins)	Peak Area (mV.s)	Peak Height (mV)
Peak 1	RI	7.56667	477069.830	9706.252

Figure S34. GPC trace of the poly(1-butene) (Table 1, Entry 6).



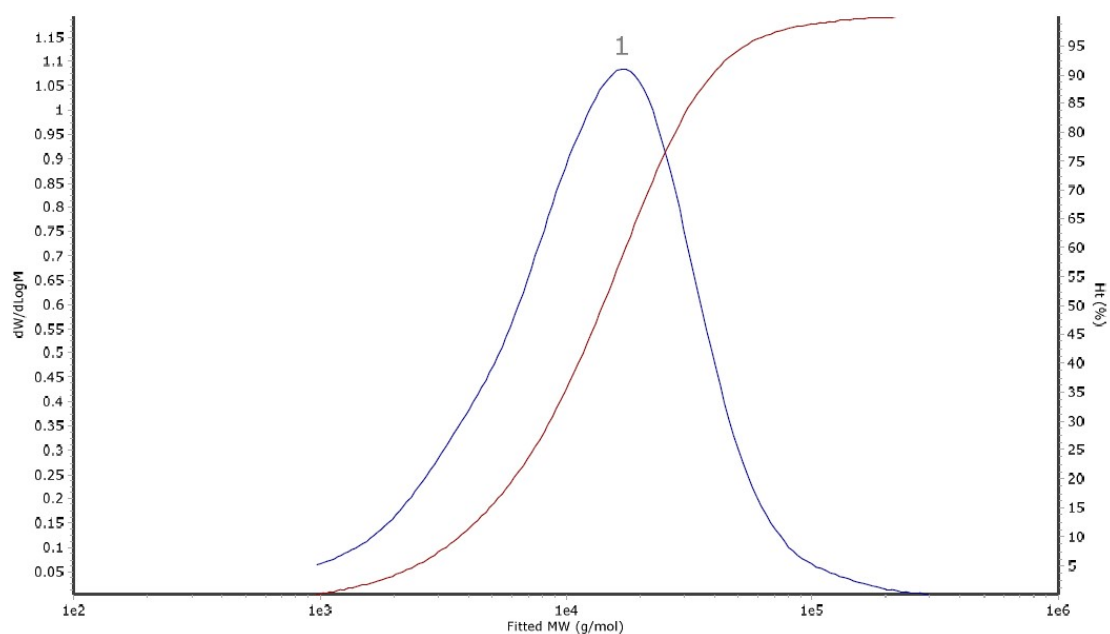
Molecular Weight Averages

Peak	Mp (g/mol)	Mn (g/mol)	Mw (g/mol)	Mz (g/mol)	Mz+1 (g/mol)	Mv (g/mol)	PD
Peak 1	15498	7445	18514	49726	128548	42435	2.487

Peak Trace Information

Peak	Trace	Peak Max RT (mins)	Peak Area (mV.s)	Peak Height (mV)
Peak 1	RI	8.25833	444656.094	8344.652

Figure S35. GPC trace of the poly(1-butene) (Table 1, Entry 7).



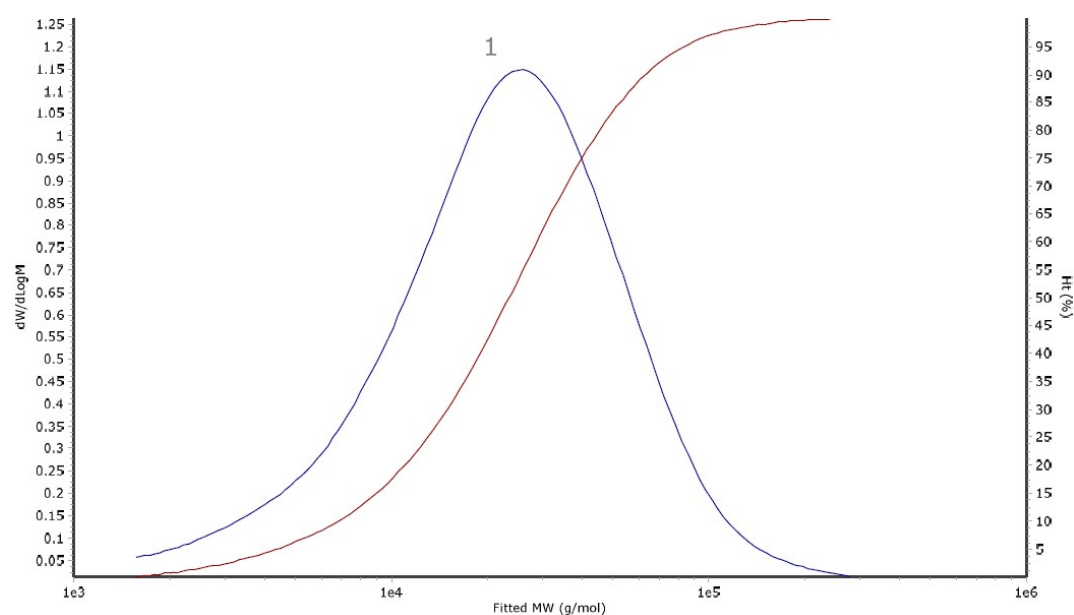
Molecular Weight Averages

Peak	Mp (g/mol)	Mn (g/mol)	Mw (g/mol)	Mz (g/mol)	Mz+1 (g/mol)	Mv (g/mol)	PD
Peak 1	17532	8314	19653	42933	89128	38181	2.364

Peak Trace Information

Peak	Trace	Peak Max RT (mins)	Peak Area (mV.s)	Peak Height (mV)
Peak 1	RI	8.20833	493998.433	9581.289

Figure S36. GPC trace of the poly(1-butene) (Table 1, Entry 8).



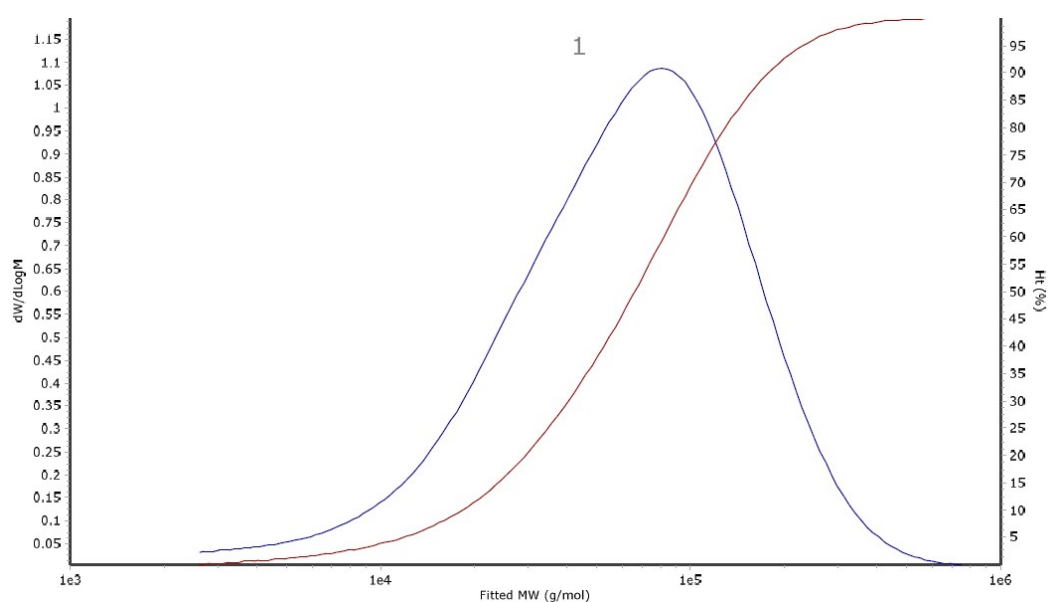
Molecular Weight Averages

Peak	Mp (g/mol)	Mn (g/mol)	Mw (g/mol)	Mz (g/mol)	Mz+1 (g/mol)	Mv (g/mol)	PD
Peak 1	26023	14407	31255	57692	96307	53057	2.169

Peak Trace Information

Peak	Trace	Peak Max RT (mins)	Peak Area (mV.s)	Peak Height (mV)
Peak 1	RI	8.04167	439712.869	9187.797

Figure S37. GPC trace of the poly(1-butene) (Table 1, Entry 9).



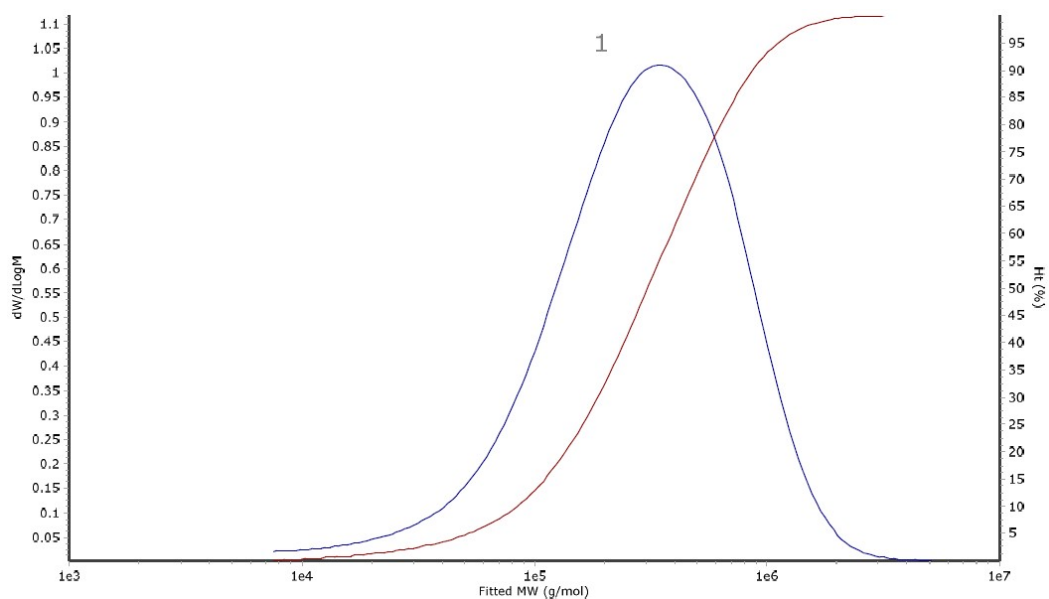
Molecular Weight Averages

Peak	Mp (g/mol)	Mn (g/mol)	Mw (g/mol)	Mz (g/mol)	Mz+1 (g/mol)	Mv (g/mol)	PD
Peak 1	82325	37541	86255	150745	228960	140580	2.298

Peak Trace Information

Peak	Trace	Peak Max RT (mins)	Peak Area (mV.s)	Peak Height (mV)
Peak 1	RI	7.60000	505034.052	10313.134

Figure S38. GPC trace of the poly(1-butene) (Table 1, Entry 10 or Table 2, Entry 1).



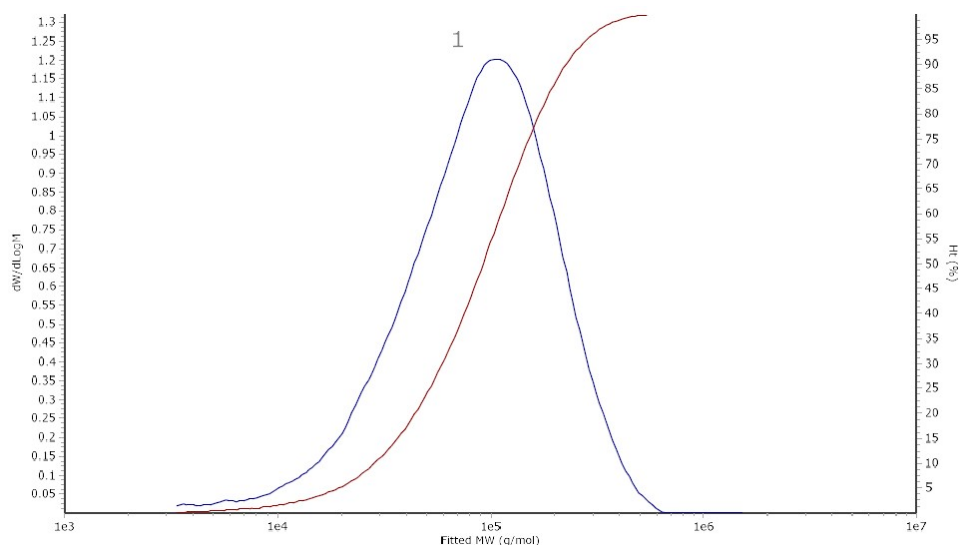
Molecular Weight Averages

Peak	Mp (g/mol)	Mn (g/mol)	Mw (g/mol)	Mz (g/mol)	Mz+1 (g/mol)	Mv (g/mol)	PD
Peak 1	347450	163152	415028	754216	1214197	698860	2.544

Peak Trace Information

Peak	Trace	Peak Max RT (mins)	Peak Area (mV.s)	Peak Height (mV)
Peak 1	RI	7.05000	665983.959	12872.983

Figure S39. GPC trace of the poly(1-butene) (Table 1, Entry 11).



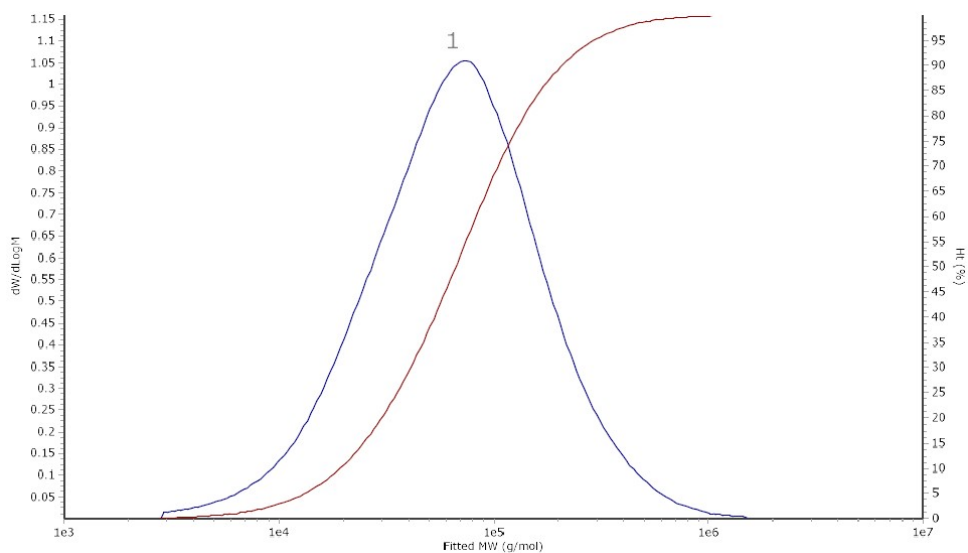
Molecular Weight Averages

Peak	Mp (g/mol)	Mn (g/mol)	Mw (g/mol)	Mz (g/mol)	Mz+1 (g/mol)	Mv (g/mol)
Peak 1	107381	56869	114686	179699	246039	105975
PD	2.017					

Peak Trace Information

Peak	Trace	Peak Max RT (mins)	Peak Area (mV.s)
Peak 1	RI	7.49520	4491.969
Peak Height (mV)		96.827	

Figure S40. GPC trace of the poly(1-butene) (Table 2, Entry 2).



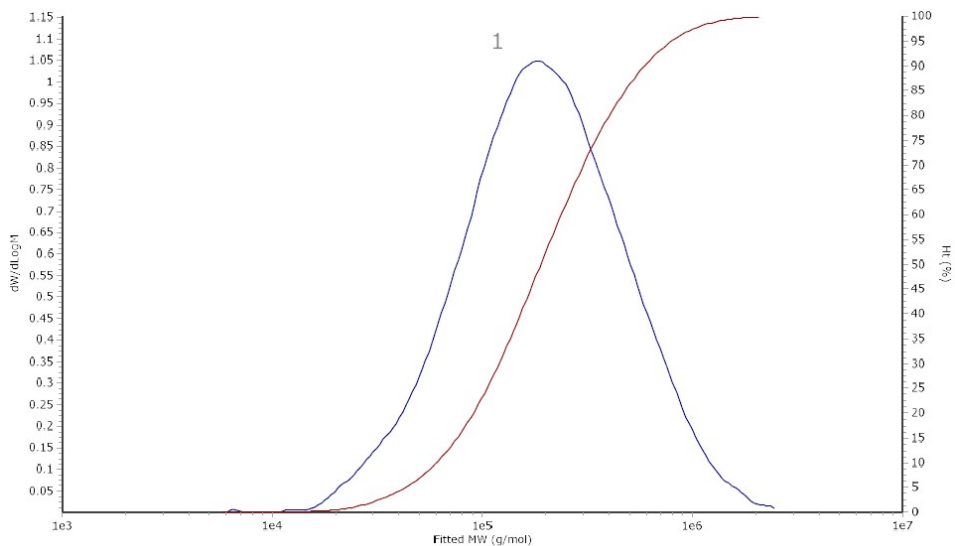
Molecular Weight Averages

Peak	Mp (g/mol)	Mn (g/mol)	Mw (g/mol)	Mz (g/mol)	Mz+1 (g/mol)	Mv (g/mol)
Peak 1	72519	41320	99663	222916	438465	87974
PD						
	2.412					

Peak Trace Information

Peak	Trace	Peak Max RT (mins)	Peak Area (mV.s)
Peak 1	RI	7.65360	31776.258
Peak Height (mV)			
		600.650	

Figure S41. GPC trace of the poly(1-butene) (Table 2, Entry 5).



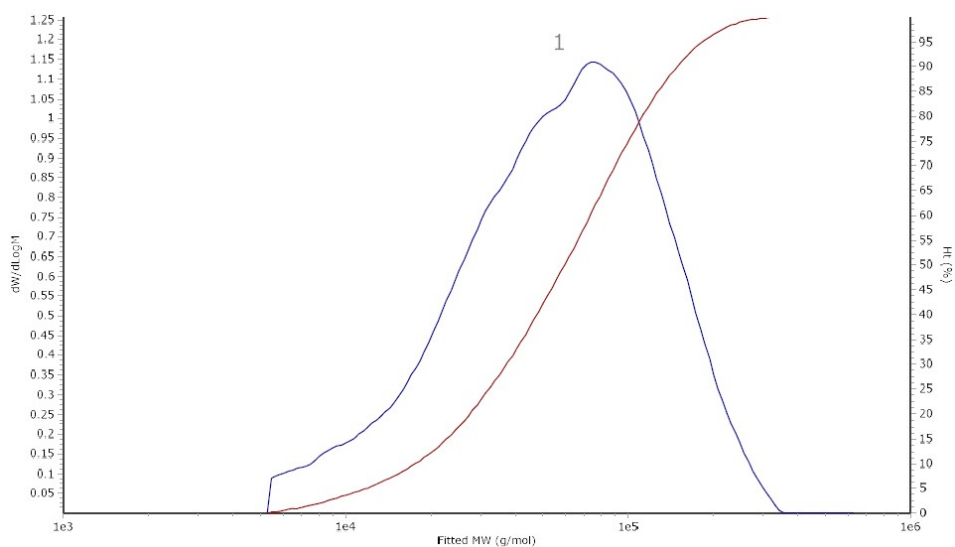
Molecular Weight Averages

Peak	Mp (g/mol)	Mn (g/mol)	Mw (g/mol)	Mz (g/mol)	Mz+1 (g/mol)	Mv (g/mol)
Peak 1	180152	129268	276827	536997	876364	248341
PD						
	2.141					

Peak Trace Information

Peak	Trace	Peak Max RT (mins)	Peak Area (mV.s)
Peak 1	RI	7.28640	4092.683
Peak Height (mV)			
		76.978	

Figure S42. GPC trace of the poly(1-butene) (Table 2, Entry 6).



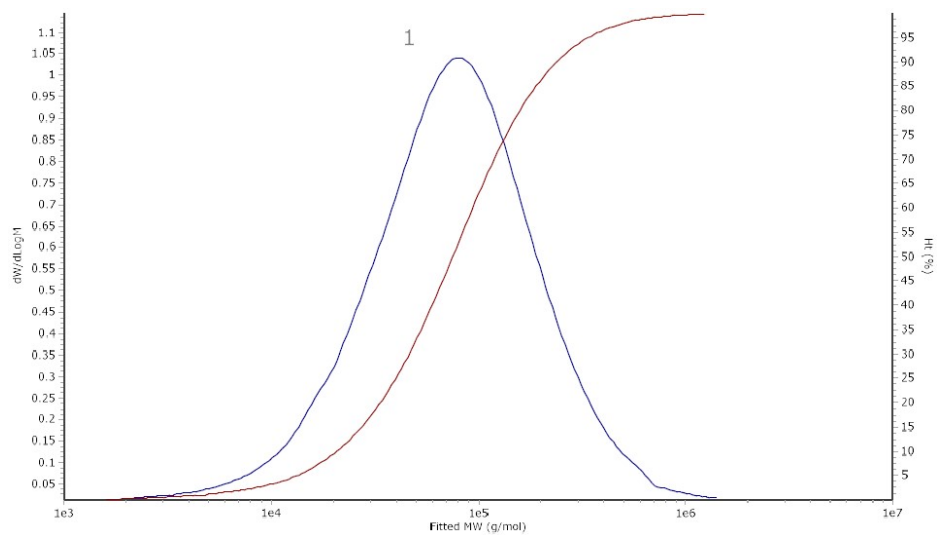
Molecular Weight Averages

Peak	Mp (g/mol)	Mn (g/mol)	Mw (g/mol)	Mz (g/mol)	Mz+1 (g/mol)	Mv (g/mol)
Peak 1	73825	38085	73867	114647	152012	68227
PD						
	1.94					

Peak Trace Information

Peak	Trace	Peak Max RT (mins)	Peak Area (mV.s)
Peak 1	RI	7.64640	1882.094
Peak Height (mV)			
		38.592	

Figure S43. GPC trace of the poly(1-butene) (Table 2, Entry 7).



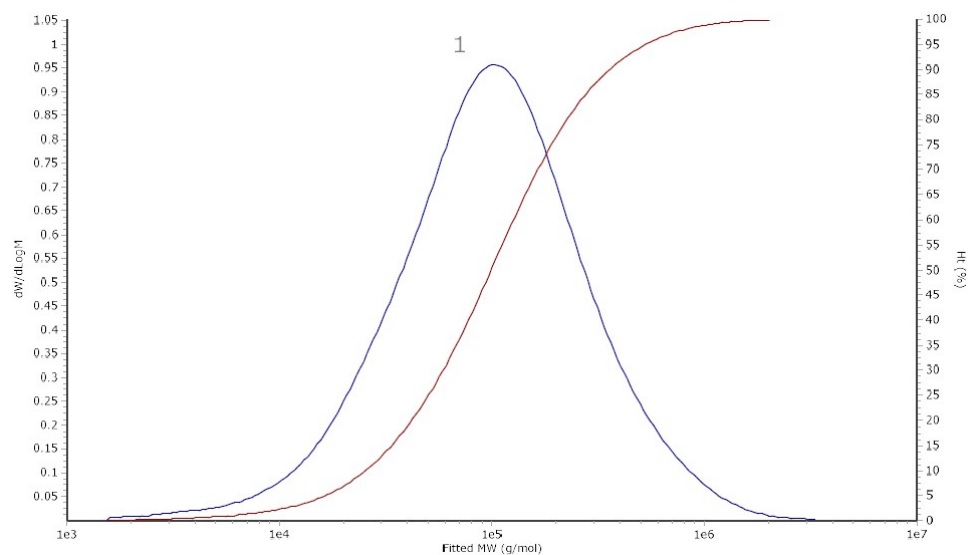
Molecular Weight Averages

Peak	Mp (g/mol)	Mn (g/mol)	Mw (g/mol)	Mz (g/mol)	Mz+1 (g/mol)	Mv (g/mol)
Peak 1	79286	40990	114611	266912	526811	100424
PD						
	2.796					

Peak Trace Information

Peak	Trace	Peak Max RT (mins)	Peak Area (mV.s)
Peak 1	RI	7.61760	28014.612
Peak Height (mV)			
		522.960	

Figure S44. GPC trace of the poly(1-butene) (Table 2, Entry 8).



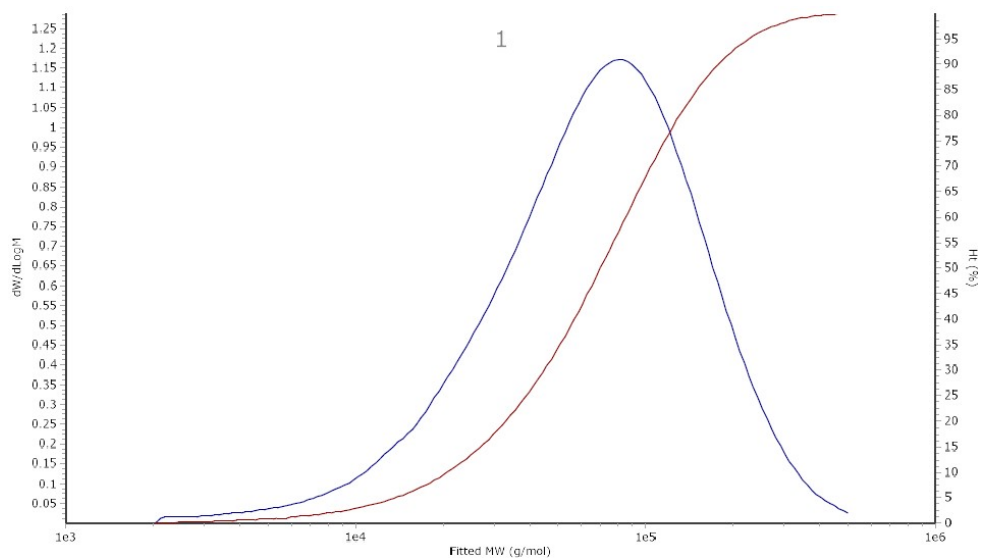
Molecular Weight Averages

Peak	Mp (g/mol)	Mn (g/mol)	Mw (g/mol)	Mz (g/mol)	Mz+1 (g/mol)	Mv (g/mol)
Peak 1	101784	52037	164707	438202	932865	141116
PD						
	3.165					

Peak Trace Information

Peak	Trace	Peak Max RT (mins)	Peak Area (mV.s)
Peak 1	RI	7.51680	28152.151
Peak Height (mV)			
		483.387	

Figure S45. GPC trace of the poly(1-butene) (Table 2, Entry 9).



Molecular Weight Averages

Peak	Mp (g/mol)	Mn (g/mol)	Mw (g/mol)	Mz (g/mol)	Mz+1 (g/mol)	Mv (g/mol)
Peak 1	80713	41615	88821	144784	204797	81553
PD						
	2.134					

Peak Trace Information

Peak	Trace	Peak Max RT (mins)	Peak Area (mV.s)
Peak 1	RI	7.61040	39335.392
Peak Height (mV)			
		826.638	

Figure S46. GPC trace of the poly(1-butene) (Table 2, Entry 10).

7. DSC Data of Polymers

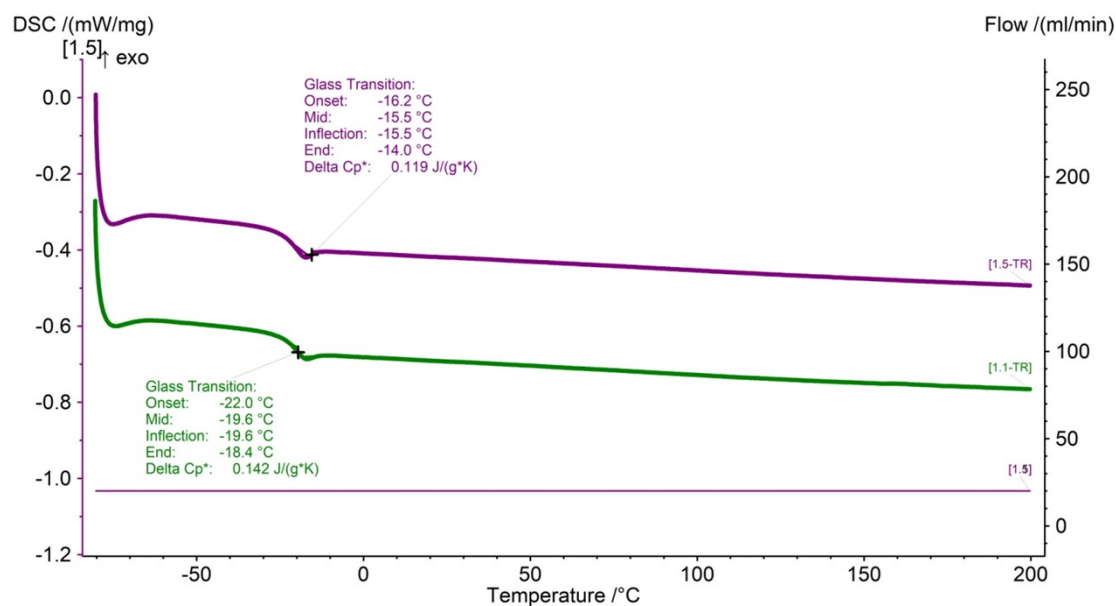


Figure S47. DSC data of the poly(1-butene) (Table 1, Entry 10 or Table 2, Entry 1).

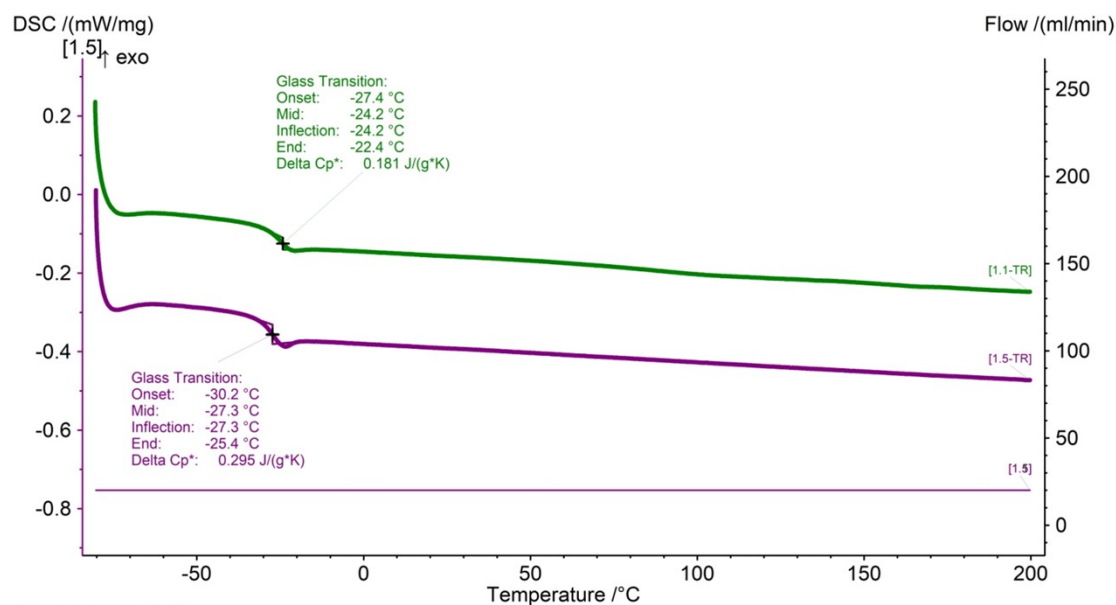


Figure S48. DSC data of the poly(1-butene) (Table 2, Entry 2).

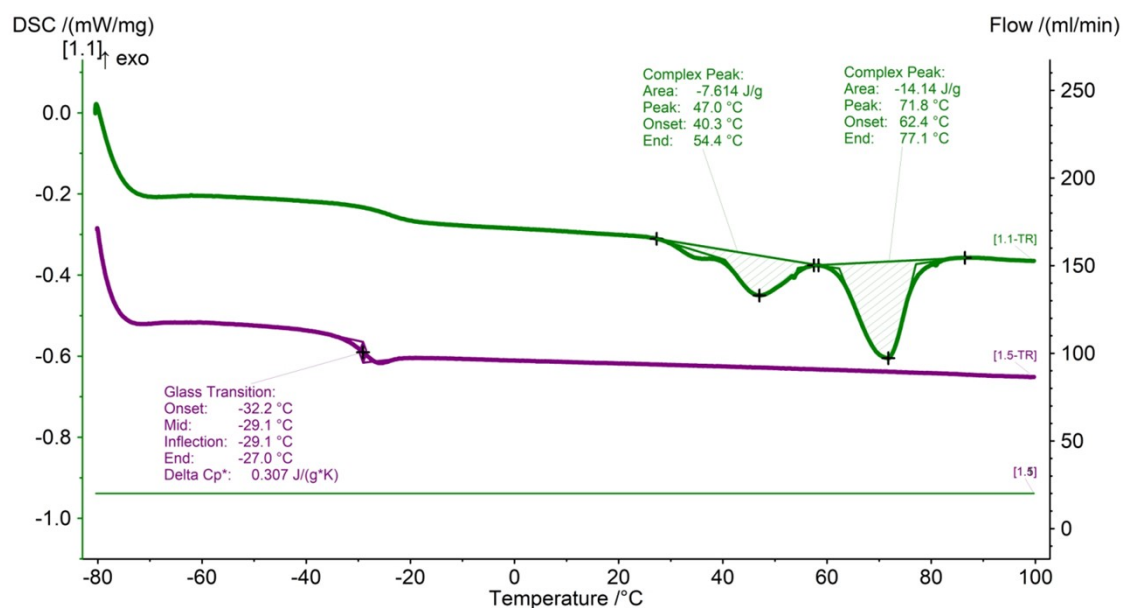


Figure S49. DSC data of the poly(1-butene) (Table 2, Entry 5).

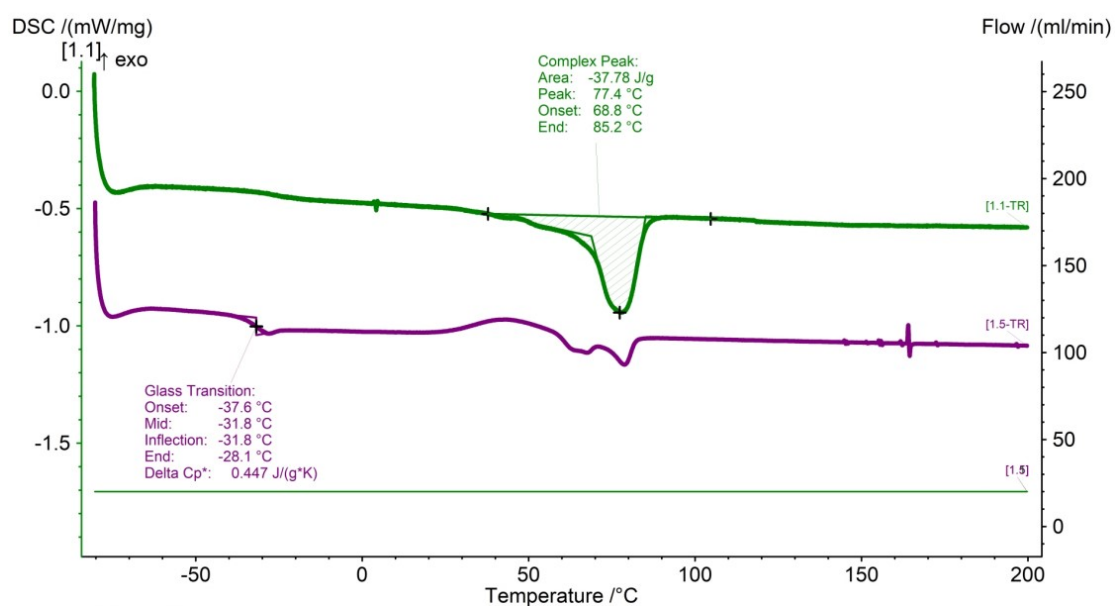


Figure S50. DSC data of the poly(1-butene) (Table 2, Entry 8).

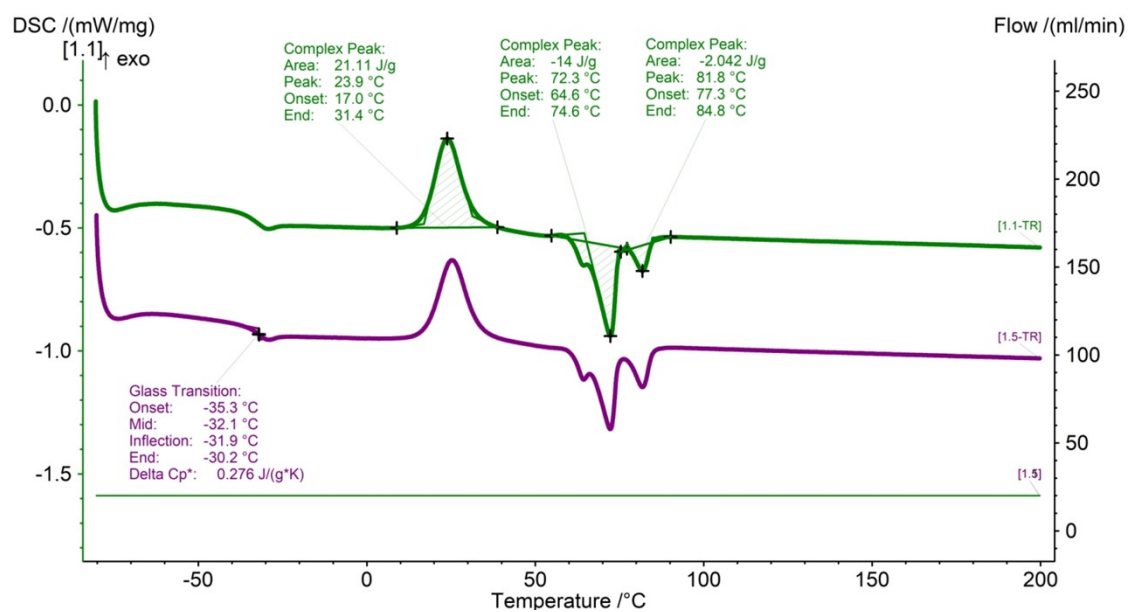


Figure S51. DSC data of the poly(1-butene) (Table 2, Entry 10).

8. WAXD data of Polymers

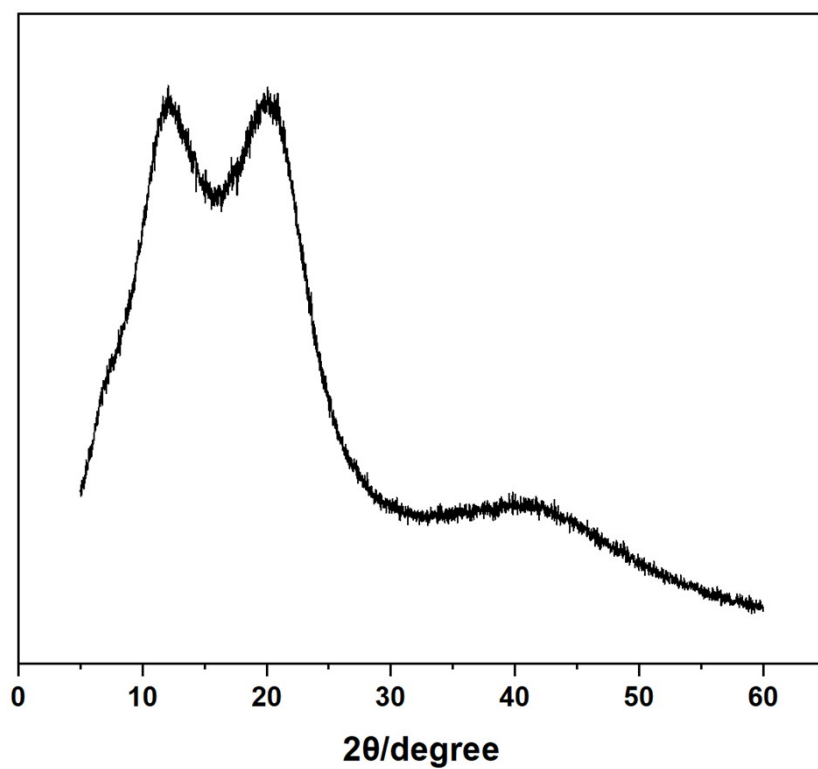


Figure S52. The WAXD spectrum of the poly(1-butene) (Table 1, Entry 10 or Table 2, Entry 1).

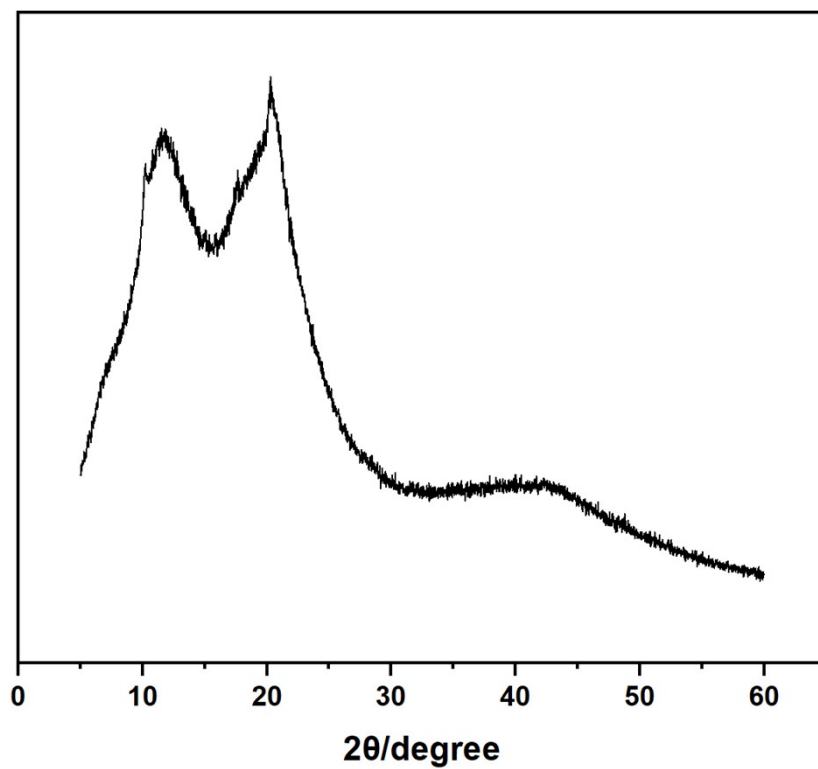


Figure S53. The WAXD spectrum of the poly(1-butene) (Table 2, Entry 2).

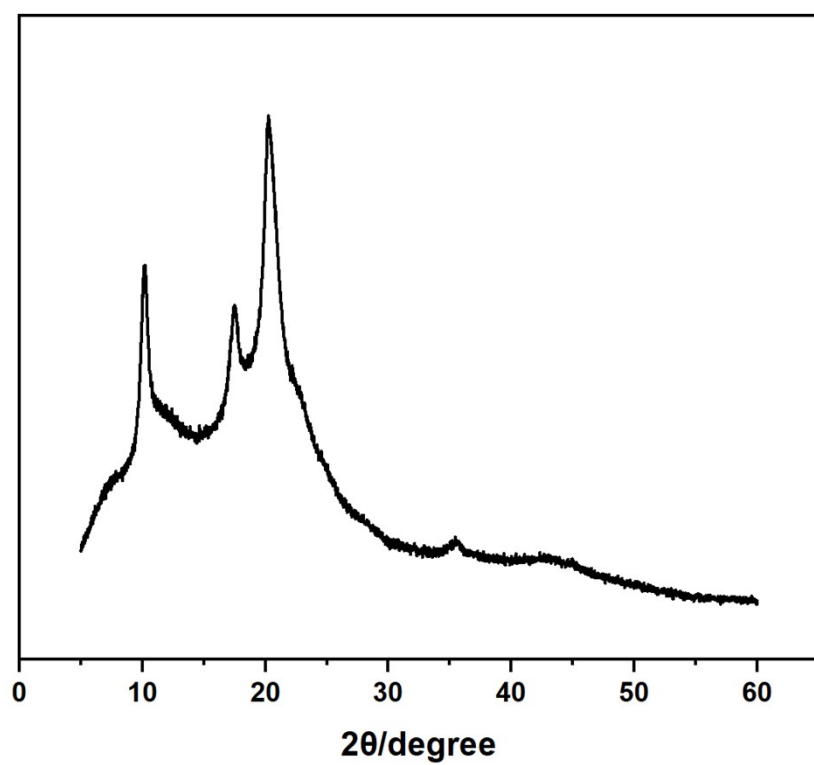


Figure S54. The WAXD spectrum of the poly(1-butene) (Table 2, Entry 5).

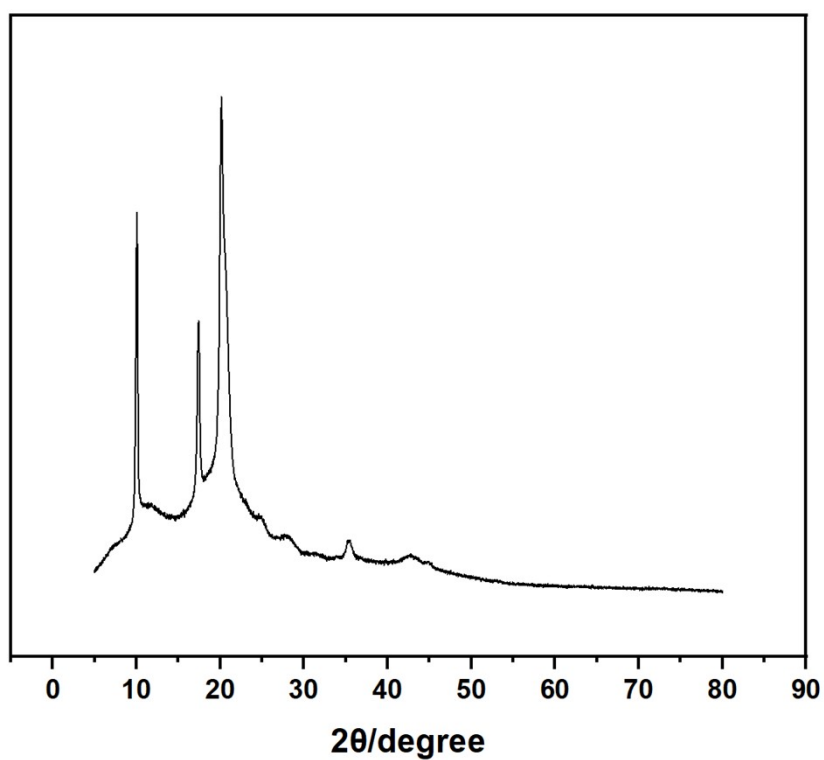


Figure S55. The WAXD spectrum of the poly(1-butene) (Table 2, Entry 8).

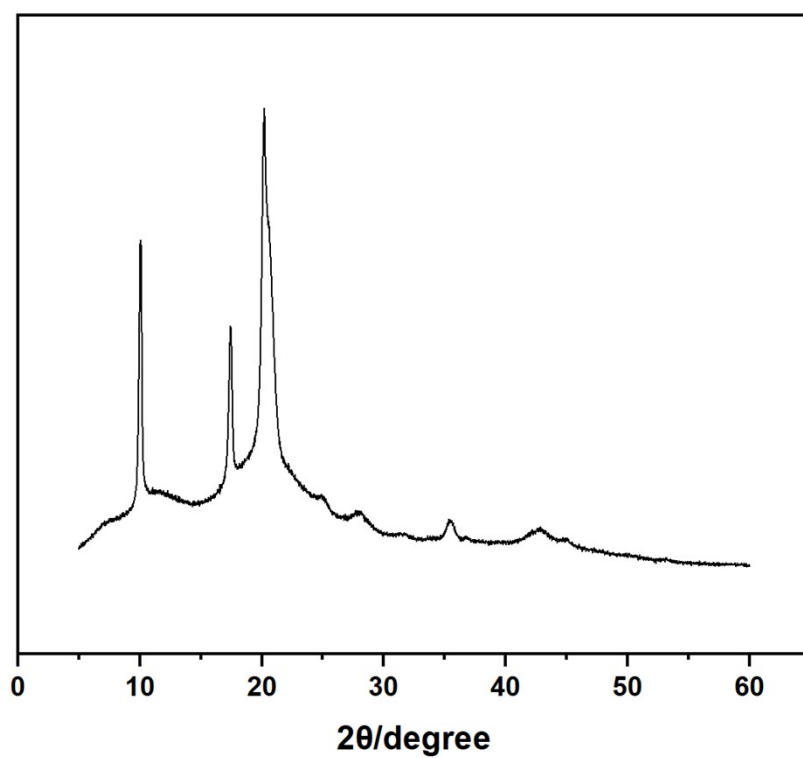


Figure S56. The WAXD spectrum of the poly(1-butene) (Table 2, Entry 10).

9. Tensile-tests of Polymers

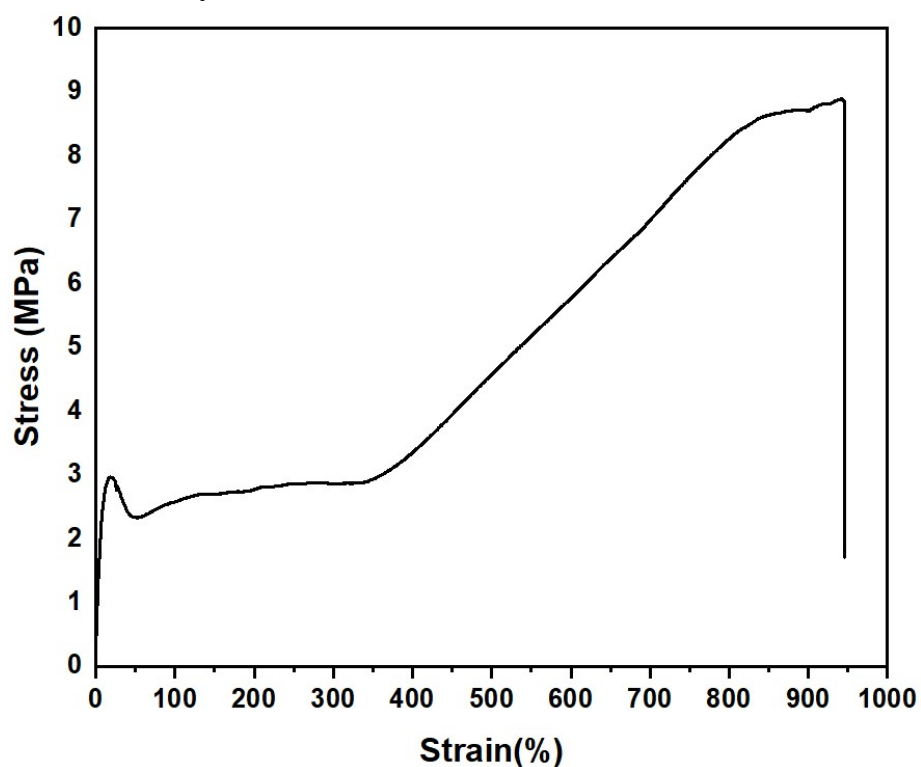


Figure S57. Tensile stress-strain curves for poly(1-butene) (Table 2, Entry 5). Yield stress = 2.9 MPa. Stress at break = 8.9 MPa, 946%.

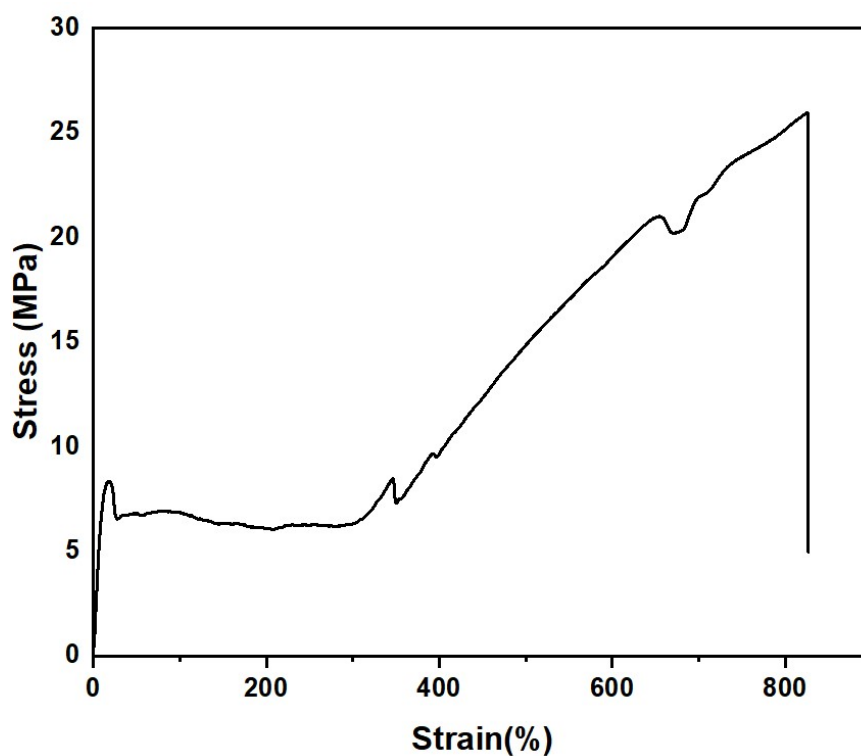


Figure S58. Tensile stress-strain curves for poly(1-butene) (Table 2, Entry 8). Yield stress = 8.3 MPa. Stress at break = 26.0 MPa, 837%.

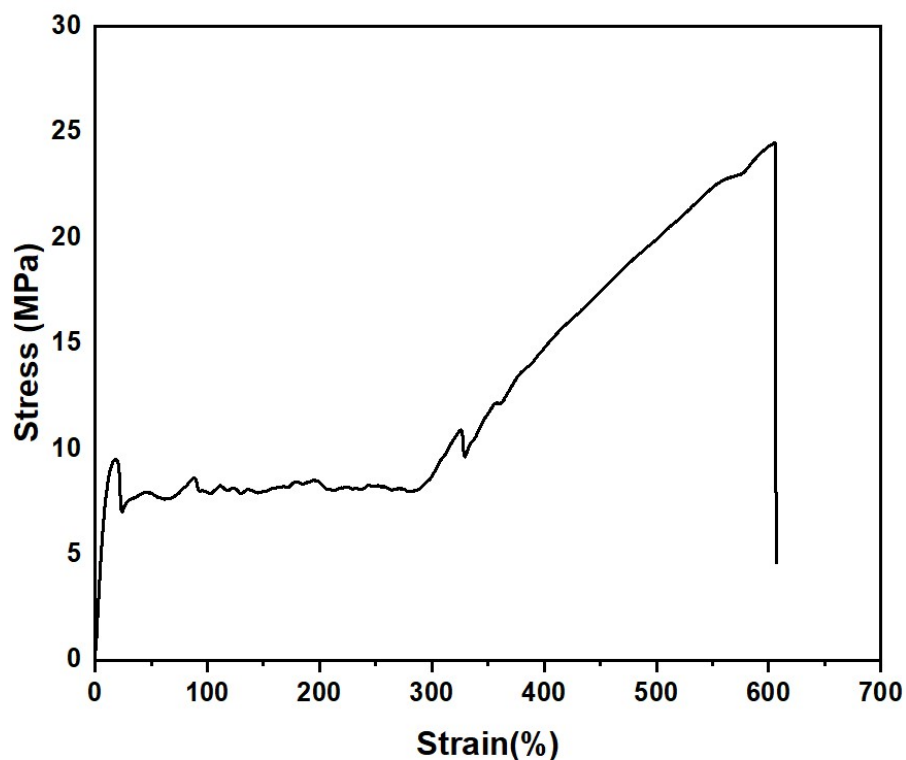


Figure S59. Tensile stress-strain curves for poly(1-butene) (Table 2, Entry 10). Yield stress = 9.5 MPa. Stress at break = 20.5 MPa, 513%.

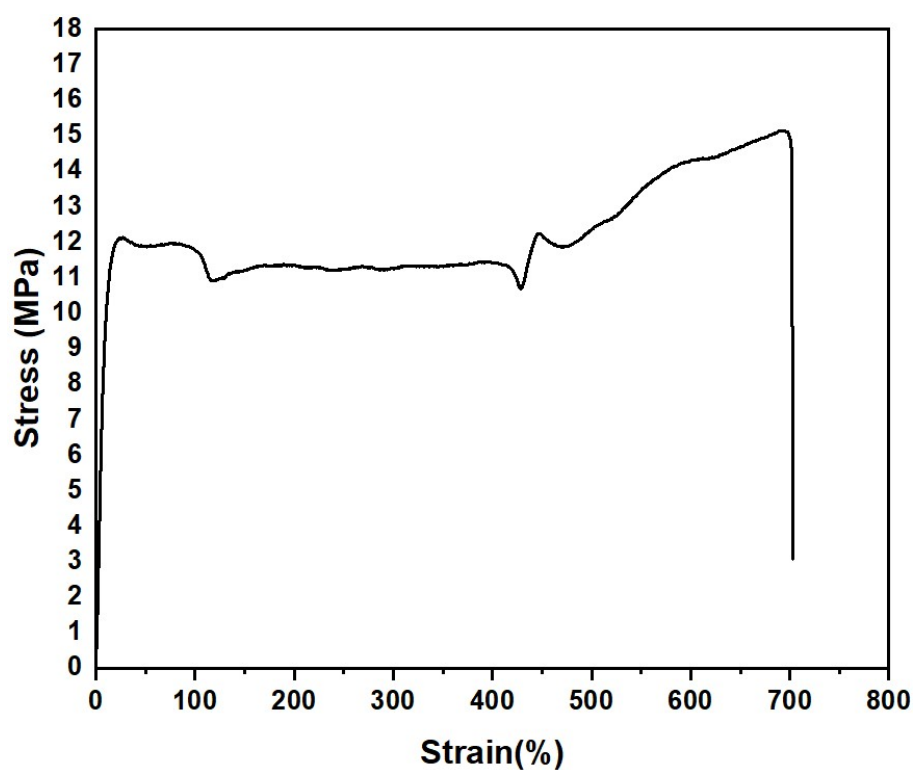
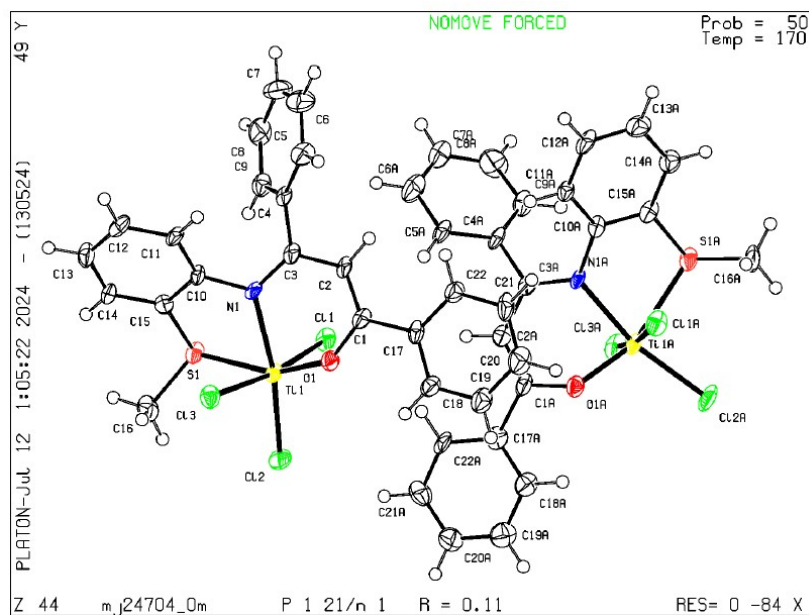


Figure S60. Tensile stress-strain curves for commercial LDPE. Yield stress = 12.1 MPa. Stress at break = 15.1 MPa, 703%.

10. Crystal Data

X-ray Structure of Complex **6a**. CCDC Number = 2412497.



Bond precision: C-C = 0.0140 Å

Wavelength=1.34139

Cell: a=23.9688(16) b=8.5432(6) c=30.1063(18)
alpha=90 beta=113.366(3) gamma=90
Temperature: 170 K

	Calculated	Reported
Volume	5659.3(7)	5659.3(7)
Space group	P 21/n	P 1 21/n 1
Hall group	-P 2yn	-P 2yn
Moiety formula	C22 H18 Cl3 N O S Ti [+ solvent]	C22 H18 Cl3 N O S Ti
Sum formula	C22 H18 Cl3 N O S Ti [+ solvent]	C22 H18 Cl3 N O S Ti
Mr	498.65	498.68
Dx, g cm ⁻³	1.171	1.171
Z	8	8
Mu (mm ⁻¹)	3.988	3.988
F000	2032.0	2032.0
F000'	2047.81	
h, k, lmax	29, 10, 36	29, 10, 36
Nref	10803	10739
Tmin, Tmax	0.533, 0.819	0.273, 0.751
Tmin'	0.483	

Correction method= # Reported T Limits: Tmin=0.273 Tmax=0.751
AbsCorr = MULTI-SCAN

Data completeness= 0.994

Theta(max)= 54.955

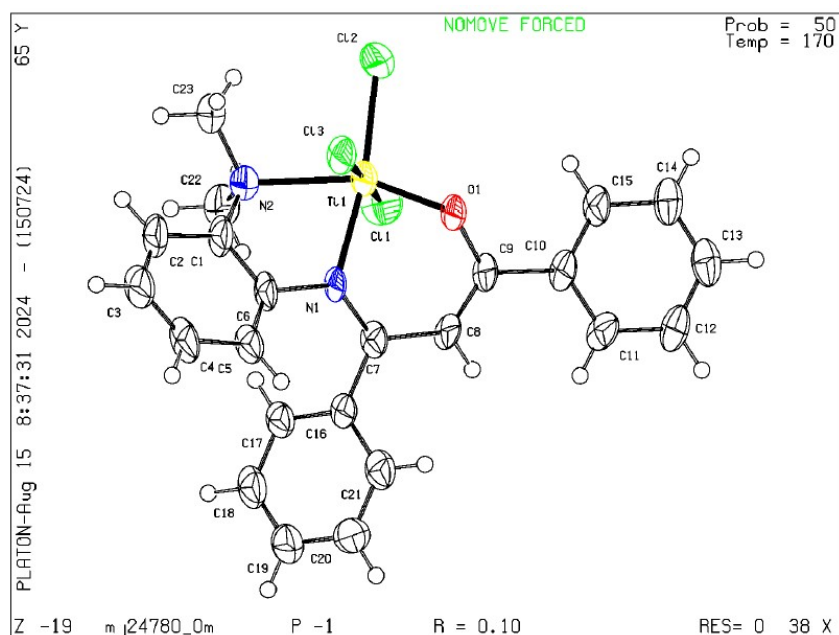
R(reflections)= 0.1138(8265)

wR2(reflections)=
0.2766(10739)

S = 1.140

Npar= 526

X-ray Structure of Complex **6c**. CCDC Number = 2412499.



Bond precision: C-C = 0.0121 Å

Wavelength=1.34139

Cell: a=8.607(2) b=9.769(3) c=14.479(4)
 alpha=99.660(12) beta=99.136(12) gamma=105.067(13)
 Temperature: 170 K

	Calculated	Reported
Volume	1132.4(5)	1132.5(5)
Space group	P -1	P -1
Hall group	-P 1	-P 1
Moiety formula	C23 H21 Cl3 N2 O Ti	C23 H21 Cl3 N2 O Ti
Sum formula	C23 H21 Cl3 N2 O Ti	C23 H21 Cl3 N2 O Ti
Mr	495.64	495.67
Dx, g cm ⁻³	1.454	1.454
Z	2	2
Mu (mm ⁻¹)	4.430	4.430
F000	508.0	508.0
F000'	511.42	
h, k, lmax	10, 11, 17	10, 11, 17
Nref	4363	4284
Tmin, Tmax	0.542, 0.801	0.251, 0.751
Tmin'	0.409	

Correction method= # Reported T Limits: Tmin=0.251 Tmax=0.751
 AbsCorr = MULTI-SCAN

Data completeness= 0.982

Theta(max)= 55.274

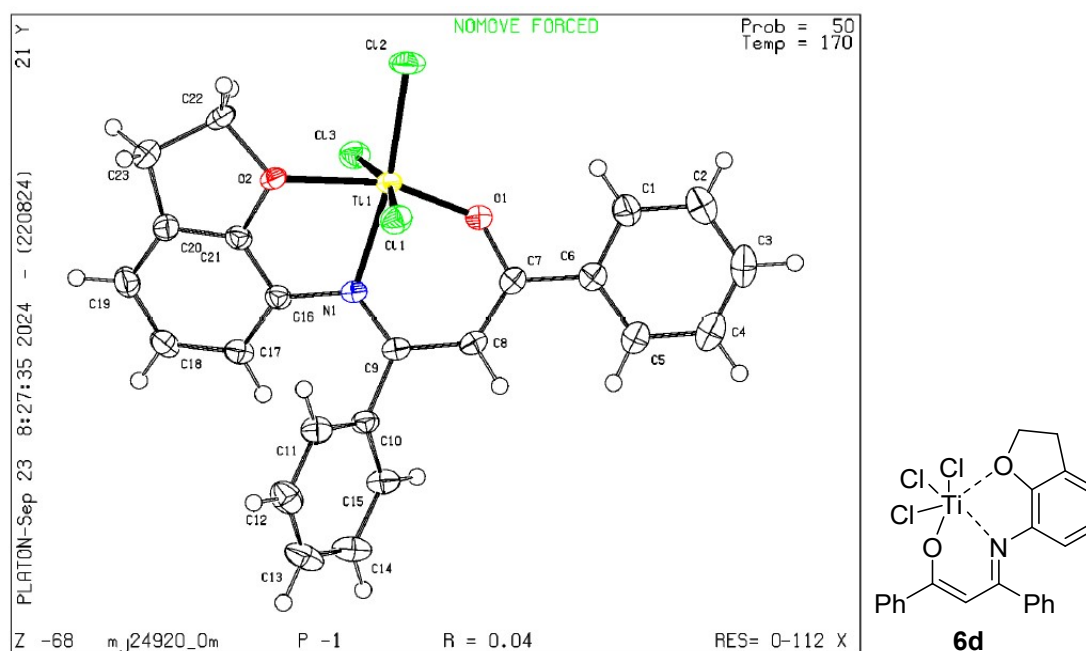
R(reflections)= 0.0996(2150)

wR2(reflections)=
0.3127(4284)

S = 1.000

Npar= 273

X-ray Structure of Complex **6d**. CCDC Number = 2412500.



Bond precision: C-C = 0.0036 Å

Wavelength=1.34139

Cell: a=9.8830 (3) b=11.2698 (3) c=14.4470 (4)
 alpha=105.467 (1) beta=94.575 (1) gamma=115.251 (1)
 Temperature: 170 K

	Calculated	Reported
Volume	1367.64 (7)	1367.63 (7)
Space group	P -1	P -1
Hall group	-P 1	-P 1
Moiety formula	C23 H18 Cl3 N O2 Ti [+ solvent]	0.5(C23 H18 Cl3 N O2 Ti)
Sum formula	C23 H18 Cl3 N O2 Ti [+ solvent]	C11.50 H9 Cl1.50 N0.50 O Ti0.50
Mr	494.60	247.32
Dx, g cm ⁻³	1.201	1.201
Z	2	4
Mu (mm ⁻¹)	3.680	3.680
F000	504.0	504.0
F000'	507.46	
h, k, lmax	12, 13, 17	12, 13, 17
Nref	5221	5108
Tmin, Tmax	0.562, 0.832	0.544, 0.751
Tmin'	0.509	

Correction method= # Reported T Limits: Tmin=0.544 Tmax=0.751
 AbsCorr = MULTI-SCAN

Data completeness= 0.978

Theta(max)= 55.008

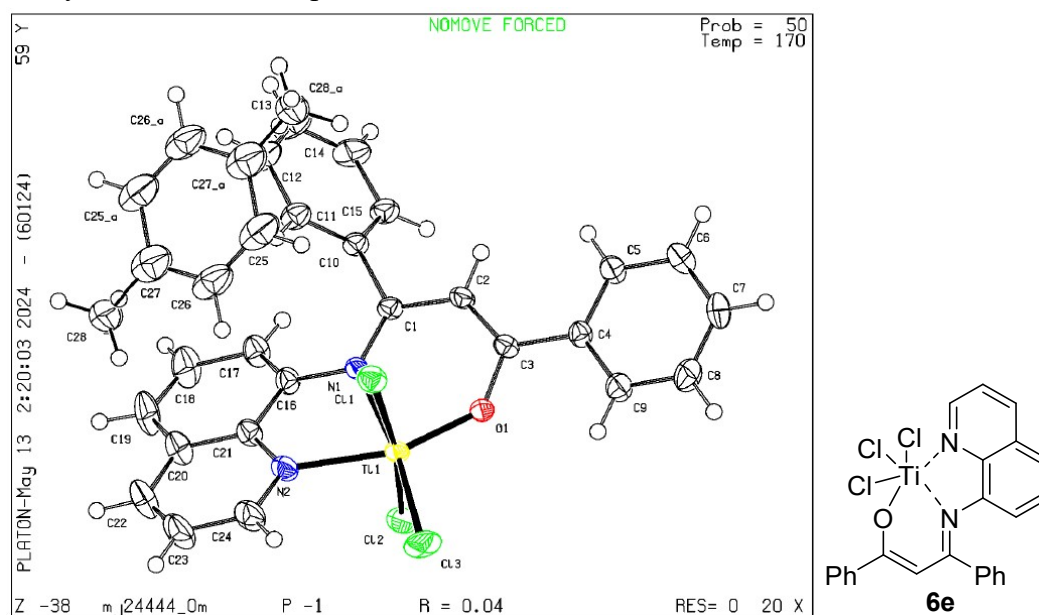
R(reflections)= 0.0391 (4820)

wR2(reflections)=
0.1105 (5108)

S = 1.060

Npar= 271

X-ray Structure of Complex **6e**. CCDC Number = 2412502.



Bond precision: C-C = 0.0037 Å

Wavelength=1.34139

Cell: a=9.7237 (2) b=11.7183 (3) c=14.3455 (3)
 alpha=108.652 (1) beta=109.153 (1) gamma=92.134 (1)
 Temperature: 170 K

	Calculated	Reported
Volume	1444.45 (6)	1444.44 (6)
Space group	P -1	P -1
Hall group	-P 1	-P 1
Moiety formula	2(C24 H17 Cl3 N2 O Ti), C7 H8 [+ solvent]	C24 H17 Cl3 N2 O Ti, C3.5 H4
Sum formula	C55 H42 Cl6 N4 O2 Ti2 [+ solvent]	C27.50 H21 Cl3 N2 O Ti
Mr	1099.37	549.71
Dx, g cm ⁻³	1.264	1.264
Z	1	2
Mu (mm ⁻¹)	3.509	3.509
F000	562.0	562.0
F000'	565.53	
h, k, lmax	11, 14, 17	11, 14, 17
Nref	5501	5464
Tmin, Tmax	0.578, 0.839	0.429, 0.751
Tmin'	0.524	

Correction method= # Reported T Limits: Tmin=0.429 Tmax=0.751
 AbsCorr = MULTI-SCAN

Data completeness= 0.993 Theta(max)= 54.921

R(reflections)= 0.0389 (4677) wR2(reflections)=
 0.1064 (5464)
 S = 1.070 Npar= 317

References:

1. A. Rossi, *Macromolecules* 1995, **28**, 1739.
2. Q. Huang, Q. Wu, F. Zhu, S. Lin, *J. Polym. Sci. Part A: Polym. Chem.* 2001, **39**, 4068.
3. M. J. Frisch, G. W. Trucks, H. B. Schlegel, G. E. Scuseria, M. A. Robb, J. R. Cheeseman, G. Scalmani, V. Barone, G. A. Petersson, H. Nakatsuji, X. Li, M. Caricato, A. V. Marenich, J. Bloino, B. G. Janesko, R. Gomperts, B. Mennucci, H. P. Hratchian, J. V. Ortiz, A. F. Izmaylov, J. L. Sonnenberg, D. Williams-Young, F. Ding, F. Lipparini, F. Egidi, J. Goings, B. Peng, A. Petrone, T. Henderson, D. Ranasinghe, V. G. Zakrzewski, J. Gao, N. Rega, G. Zheng, W. Liang, M. Hada, M. Ehara, K. Toyota, R. Fukuda, J. Hasegawa, M. Ishida, T. Nakajima, Y. Honda, O. Kitao, H. Nakai, T. Vreven, K. Throssell, J. A. Montgomery, Jr., J. E. Peralta, F. Ogliaro, M. J. Bearpark, J. J. Heyd, E. N. Brothers, K. N. Kudin, V. N. Staroverov, T. A. Keith, R. Kobayashi, J. Normand, K. Raghavachari, A. P. Rendell, J. C. Burant, S. S. Iyengar, J. Tomasi, M. Cossi, J. M. Millam, M. Klene, C. Adamo, R. Cammi, J. W. Ochterski, R. L. Martin, K. Morokuma, O. Farkas, J. B. Foresman, D. J. Fox, *Gaussian 16, Revision B.01*, Gaussian, Inc., Wallingford CT, 2016.
4. A. D. Becke, *Phys. Rev. A*. 1988, **38**, 3098.
5. C. Lee, W. Yang, R. G. Parr, *Phys. Rev. B*. 1988, **37**, 785.
6. S. Grimme, J. Antony, S. Ehrlich, H. Krieg, *J. Chem. Phys.* 2010, **132**, 154104.
7. A. D. McLean, G. S. Chandler, *J. Chem. Phys.* 1980, **72**, 5639.
8. R. Krishnan, J. S. Binkley, R. Seeger, J. A. Pople, *J. Chem. Phys.* 1980, **72**, 650.
9. R. C. Binning, L. A. Curtiss, *J. Comput. Chem.* 1990, **11**, 1206.
10. L. Falivene, R. Credendino, A. Poater, A. Petta, L. Serra, R. Oliva, V. Scarano, L. Cavallo, *Organometallics* 2016, **35**, 2286.
11. Z. Chen, J.-F. Li, W.-J. Tao, X.-L. Sun, X.-H. Yang, Y. Tang, *Macromolecules* 2013, **46**, 2870.